
BIOSCAN-5M: A Multimodal Dataset for Insect Biodiversity

Zahra Gharaee^{2*}, Scott C. Lowe^{4*}, ZeMing Gong^{3*}, Pablo Millan Arias^{2*},
Nicholas Pellegrino², Austin T. Wang³, Joakim Bruslund Haurum⁶,
Iuliia Zarubiieva^{1,4}, Lila Kari²,
Dirk Steinke^{1†}, Graham W. Taylor^{1,4†}, Paul Fieguth^{2†}, Angel X. Chang^{3,5†}
¹University of Guelph, ²University of Waterloo, ³Simon Fraser University,
⁴Vector Institute, ⁵Alberta Machine Intelligence Institute (Amii),
⁶Aalborg University and Pioneer Centre for AI
<https://biodiversitygenomics.net/5M-insects/>

Abstract

As part of an ongoing worldwide effort to comprehend and monitor insect biodiversity, this paper presents the BIOSCAN-5M Insect dataset to the machine learning community and establish several benchmark tasks. BIOSCAN-5M is a comprehensive dataset containing multi-modal information for over 5 million insect specimens, and it significantly expands existing image-based biological datasets by including taxonomic labels, raw nucleotide barcode sequences, assigned barcode index numbers, and geographical information. We propose three benchmark experiments to demonstrate the impact of the multi-modal data types on the classification and clustering accuracy. First, we pretrain a masked language model on the DNA barcode sequences of the BIOSCAN-5M dataset, and demonstrate the impact of using this large reference library on species- and genus-level classification performance. Second, we propose a zero-shot transfer learning task applied to images and DNA barcodes to cluster feature embeddings obtained from self-supervised learning, to investigate whether meaningful clusters can be derived from these representation embeddings. Third, we benchmark multi-modality by performing contrastive learning on DNA barcodes, image data, and taxonomic information. This yields a general shared embedding space enabling taxonomic classification using multiple types of information and modalities. The code repository of the BIOSCAN-5M Insect dataset is available at <https://github.com/zahrag/BIOSCAN-5M>

1 Introduction

Biodiversity plays a multifaceted role in sustaining ecosystems and supporting human well-being. Primarily, it serves as a cornerstone for ecosystem stability and resilience, providing a natural defence against disturbances such as climate change and invasive species [9]. Additionally, biodiversity serves as a vital resource for the economy, supplying essentials like food, medicine, and genetic material [65]. Understanding biodiversity is paramount for sustainable resource management, ensuring the availability of these resources for future generations [18].

Expanding upon the BIOSCAN-1M Insect dataset [23], we introduce the BIOSCAN-5M dataset — a comprehensive repository containing multi-modal information (Figure 1) on over 5 million arthropod specimens, 98% of which are insects. Compared to its predecessor, the BIOSCAN-5M dataset offers a significantly larger volume of high-resolution microscope images and DNA barcodes along with critical annotations, including taxonomic ranks, and geographical location.

*Joint first author. †Joint senior/last author.

Biological Taxonomy		Genetic Information		RGB Image		Size information		Geographical Information	
Phylum	Arthropoda	DNA Barcode Sequence		Original Image	Cropped Image	Meas.Value	64,331	Country	United States
Class	Insect	TATTATATTCATTTTCGC ...						Province/State	California
Order	Hymenoptera	Barcode Index Number				Scale Factor	2.08	Latitude	40.10132
Family	Formicidae	BOLD:AAA3908				Area Fraction	0.44	Longitude	-122.05354
Subfamily	Dolichoderinae								
Genus	Tapinoma								
Species	Tapinoma sessile								

Figure 1: The BIOSCAN-5M Insect Dataset provides taxonomic labels, a high-resolution image, size information (from automatic crops), a DNA barcode, barcode index number, and geographic location for each sample.

The multimodal characteristics inherent to the BIOSCAN-5M dataset are not only essential for biodiversity studies but also facilitate further innovation in machine learning and artificial intelligence. In this paper, we design and implement experiments to leverage the multimodal aspects of the BIOSCAN-5M dataset, extending its application beyond the image modality used in [23]. First, we train the masked language model (MLM) proposed in BarcodeBERT [52] on the DNA barcodes of the BIOSCAN-5M dataset and demonstrate the impact of using this large reference library on species- and genus-level classification. We achieve with our model an accuracy higher than that of state-of-the-art models pretrained on more general genomic datasets, especially in the 1NN-probing task of assigning samples from unseen species to seen genera. Next, we perform a zero-shot transfer learning task [47] through zero-shot clustering representation embeddings obtained from encoders trained with self-supervised paradigms. This approach demonstrates the effectiveness of pretrained embeddings in clustering data, even in the absence of ground-truth. Finally, we learn a shared embedding space across three modalities in the dataset as in BIOSCAN-CLIP [24], including high-quality RGB images, textual taxonomic labels, and DNA barcodes, for fine-grained taxonomic classification.

2 Related work

2.1 Datasets for taxonomic classification

Biological datasets are essential for advancing our understanding of the natural world, with uses in genomics [55], proteomics [41], ecology [40], evolutionary biology [20], medicine [37], and agriculture [50, 82, 21, 30]. Table 1 compares biological datasets used for taxonomic classification. Many of these datasets feature fine-grained classes and exhibit a long-tailed class distribution, making the recognition task challenging for machine learning (ML) methods that do not account for these properties. While many datasets provide images, they do not include other attributes such as DNA barcode, or geographical locations. Most relevant to our work is BIOSCAN-1M Insect [23], which introduced a dataset of 1.1 M insect images paired with DNA barcodes and taxonomic labels.

DNA barcodes are short, highly descriptive DNA fragments that encode sufficient information for species-level identification. For example, a DNA barcode of an organism from Kingdom Animalia [31, 7] is a specific 648 bp sequence of the cytochrome c oxidase I (COI) gene from the mitochondrial genome, used to classify unknown individuals and discover new species [54]. DNA barcodes have been successfully applied to taxonomic identification and classification, ecology, conservation, diet analysis, and food safety [63, 73], offering faster and more accurate results than traditional methods [59]. Barcodes can also be grouped together based on sequence similarity into clusters called Operational Taxonomic Units (OTUs) [69, 6], each assigned a Barcode Index Number (BIN) [62]. In general, biological datasets may also incorporate other data such as labels for multi-level taxonomic ranks, which can offer valuable insights into the evolutionary relationships between organisms. However, datasets with hierarchical taxonomic annotations [30, 35, 45, 81, 23] are relatively scarce.

2.2 Self-supervised learning

Self-supervised learning (SSL) has recently gained significant attention for its ability to leverage vast amounts of unlabeled data, producing versatile feature embeddings for various tasks [4]. This has driven the development of large-scale language models [8] and computer vision systems trained on billions of images [25]. Advances in transformers pretrained with SSL at scale, known as foundation models [38, 85, 14, 86, 13, 26], have shown robust performance across diverse tasks.

Table 1: **Summary of fine-grained and long-tailed biological datasets.** The ‘‘Taxa’’ column indicates the taxonomic scope of each dataset. The ‘‘IR’’ column indicates the class imbalance ratio, computed as the ratio of the number of samples in the most populated category to the least populated category.

Dataset	Ref.	Year	Images	IR	Taxa	Rank	Categories	Taxonomy	BIN	DNA	Habitat	Size
LeafSnap	[43]	2012	31 k	8	Plants	Species	184	×	×	×	×	×
NA Birds	[75]	2015	48 k	15	Birds	Species	400	×	×	×	×	×
Urban Trees	[80]	2016	80 k	7	Trees	Species	18	×	×	×	×	×
DeepWeeds	[58]	2019	17 k	9	Plants	Species	9	×	×	×	✓	×
IP102	[81]	2019	75 k	14	Insects	Species	102	✓	×	×	×	×
Pest24	[79]	2020	25 k	494	Insects	Species	24	×	×	×	×	×
Pl@ntNet-300K	[22]	2021	306 k	3,604	Plants	Species	1,000	×	×	×	×	×
iNaturalist (2021)	[76]	2021	2,686 k	2	All	Species	10,000	✓	×	×	×	×
iNaturalist-Insect	[76]	2021	663 k	2	Insects	Species	2,526	✓	×	×	×	×
Species196-L	[30]	2023	19 k	351	Various	Mixed	196	✓	×	×	×	×
CWD30	[35]	2023	219 k	61	Plants	Species	30	✓	×	×	×	×
BenthicNet	[48]	2024	1,429 k	22,394	Aquatic	Mixed	791	✓	×	×	✓	×
Insect-1M	[57]	2024	1,017 k	N/A	Arthropods	Species	34,212	✓	×	×	×	×
BIOSCAN-1M	[23]	2023	1,128 k	12,491	Insects	BIN*	90,918	✓	✓	✓	×	×
BIOSCAN-5M	Ours	2024	5,150 k	35,458	Arthropods	BIN*	324,411	✓	✓	✓	✓	✓

* For datasets that include Barcode Index Numbers (BINs) annotations, we present BINs, which serve as a (sub)species proxy for organisms and offer a viable alternative to Linnean taxonomy.

Recent work has leveraged these advances for taxonomic classification using DNA. Since the introduction of the first DNA language model, DNABERT [38], which mainly focused on human data, multiple models with different architectures and tokenization strategies have emerged [53, 85, 86, 52, 56] with some incorporating data from multiple species during pretraining and allowing for species classification [85, 86, 52]. These models are pretrained to be task-agnostic, and are expected to perform well after fine-tuning in downstream tasks. Yet, their potential application for taxonomic identification of arbitrary DNA sequences or DNA barcodes has not been extensively explored. One relevant approach, BERTax [53], pretrained a BERT [16] model for hierarchical taxonomic classification on broader ranks such as kingdom, phylum, and genus. For DNA barcodes specifically, BarcodeBERT [52] was developed for species-level classification of insects, with assignment to genus for unknown species.

Although embeddings from SSL-trained feature extractors exhibit strong performance on downstream tasks post fine-tuning, their utility without fine-tuning remains underexplored. Previous studies [77, 84] suggest that SSL feature encoders produce embeddings conducive to clustering, albeit typically after fine-tuning. A recent study [47] has delved into whether SSL-trained feature encoders *without* fine-tuning can serve as the foundation for clustering, yielding informative clusters of embeddings on real-world datasets unseen during encoder training.

2.3 Multimodal Learning

There has been a growing interest in exploring multiple data modalities for biological tasks [34, 49, 83]. Badirli et al. [2] introduced a Bayesian zero-shot learning approach, leveraging DNA data to model priors for species classification based on images. Those authors also employed Bayesian techniques [3], combining image and DNA embeddings in a unified space to predict the genus of unseen species.

Recent advances in machine learning have allowed for the scalable integration of information across diverse modalities. For example, CLIP [61] used contrastive learning to encode text captions and images into a unified space for zero-shot classification. BioCLIP [72] used a similar idea to align images of organisms with their common names and taxonomic descriptions across a dataset of 10 M specimens encompassing plants, animals, and fungi. BIOSCAN-CLIP [24] used a contrastive loss to align the three modalities of RGB images, textual taxonomic labels, and DNA barcodes. By aligning these modalities, BIOSCAN-CLIP can use either images or DNA barcodes for taxonomic classification and learn from incomplete taxonomic labels, making it more flexible than BioCLIP [72], which requires full taxonomic annotations for each specimen.

3 Dataset

The BIOSCAN-5M dataset is derived from Steinke et al. [71] and comprises 5,150,850 arthropod specimens, with insects accounting for 98% of the total. The diverse features of this dataset are described in this section. The BIOSCAN-5M dataset is a superset of the BIOSCAN-1M Insect dataset [23], providing more samples and additional metadata such as geographical location.

Images. The BIOSCAN-5M dataset provides specimen images at 1024×768 pixels, captured using a Keyence VHX-7000 microscope. Figure 2 showcases the diversity in organism morphology across the dataset. The images are accessed via the `processid` field of the metadata as `{processid}.1024px.jpg`. Following BIOSCAN-1M Insect [23], the images are cropped and resized to 341×256 pixels to facilitate model training. We fine-tuned DETR (End-to-End Object Detection with Transformers) for image cropping. For BIOSCAN-1M Insect, the cropping model was trained using 2 k insect images. Building on the BIOSCAN-1M Insect cropping tool checkpoint, we fine-tuned the model for BIOSCAN-5M using the same 2 k images and an additional 837 images that were not well-cropped previously. This fine-tuning process followed the same training setup, including batch size, learning rate, and other hyper parameter settings (see supplement for details). The bounding box of the cropped region is provided as part of the dataset release.



Figure 2: Samples of original full-size images of distinct organisms in the BIOSCAN-5M dataset.

Genetic-based indexing. The genetic information of the BIOSCAN-5M dataset described in §2 is represented as the raw nucleotide barcode sequence, under the `nucraw` field, and the Barcode Index Number under `uri` field. Independently, the field `processid` is a unique number assigned by BOLD [36] to each record, and `sampleid` is an identifier given by the collector.

Biological taxonomic classification. The dataset samples undergo taxonomic classification using a hybrid approach involving an AI-assisted tool proposed by Gharaee et al. [23] and human taxonomic experts. After DNA barcoding and sequence alignment, the taxonomic levels derived from both the AI tool and DNA sequencing are compared. Any discrepancies are then reviewed by human experts. Importantly, assignments to deeper taxonomic levels, such as family or lower, rely entirely on human expertise. Labels at seven taxonomic ranks are used to represent individual specimens, denoted by fields `phylum`, `class`, `order`, `family`, `subfamily`, `genus`, and `species`.

Table 2: Summary statistics of dataset records by taxonomic rank.

Attributes	BIOSCAN-5M (Ours)				BIOSCAN-1M [23]		
	IR	Categories	Labelled	Labelled (%)	Categories	Labelled	Labelled (%)
<code>phylum</code>	1	1	5,150,850	100.0	1	1,128,313	100.0
<code>class</code>	719,831	10	5,146,837	99.9	1	1,128,313	100.0
<code>order</code>	3,675,317	55	5,134,987	99.7	16	1,128,313	100.0
<code>family</code>	938,928	934	4,932,774	95.8	491	1,112,968	98.6
<code>subfamily</code>	323,146	1,542	1,472,548	28.6	760	265,492	23.5
<code>genus</code>	200,268	7,605	1,226,765	23.8	3,441	254,096	22.5
<code>species</code>	7,694	22,622	473,094	9.2	8,355	84,397	7.5
<code>dna_bin</code>	35,458	324,411	5,137,441	99.7	91,918	1,128,313	100.0
<code>dna_barcode</code>	3,743	2,486,492	5,150,850	100.0	552,629	1,128,313	100.0

In the raw dataset, we found identical DNA nucleotide sequences labelled differently at some taxonomic levels, which was likely due to human error (e.g. typos) or disagreements in the taxonomic naming. To address this, we checked and cleaned the taxonomic labels to address typos and ensure consistency across DNA barcodes (see supplement for details). We note that some of the noisy species labels are placeholder labels that do not correspond to well-established scientific taxonomic species names. In our data, the placeholder species labels are identified by species labels that begin with a lowercase letter, contain a period, contain numerals, or contain “malaise”.

Statistics for BIOSCAN-5M are given in Table 2 for the seven taxonomic ranks along with the BIN and DNA nucleotide barcode sequences. For each group, we report the number of categories, the count and the percentage of labelled and unlabelled records. We compute the class imbalance ratio (IR) as the ratio of the number of samples in the largest category to the smallest category, reflecting the class distribution within each group.

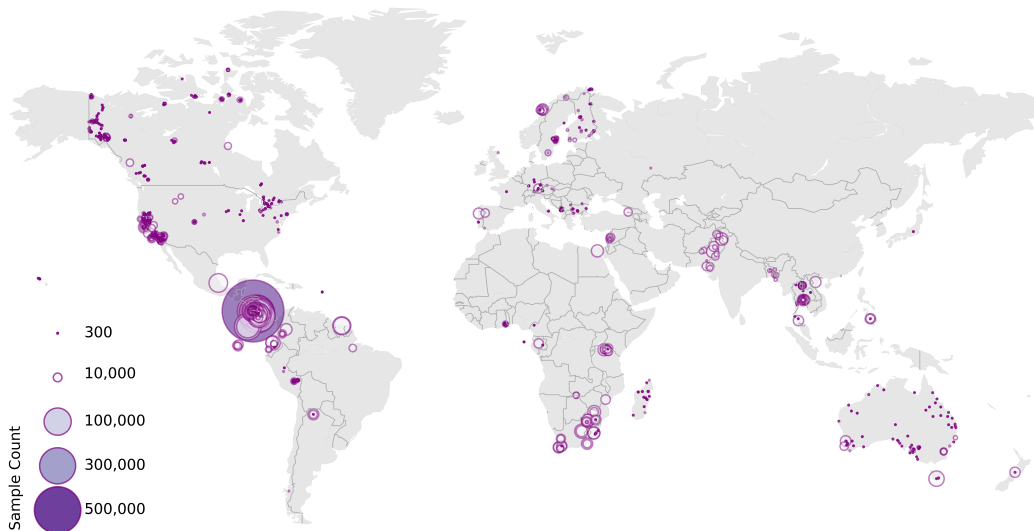


Figure 3: Geographical locations obtained from latitude and longitude coordinates of the regions where the samples of the BIOSCAN-5M dataset were collected.

Geographic location. The BIOSCAN-5M dataset provides geographic location information, detailing the country and province or state where each specimen is collected, along with the latitude and longitude coordinates of each collection site. This information is detailed in the fields `country`, `province/state`, `coord-lat` and `coord-lon`. The distribution of specimen collection sites are shown on a world map in Figure 3.

Challenges. The BIOSCAN-5M dataset faces two key challenges: First, there exists a sampling bias as a result of the locations where and the methods through which specimens are collected. Second, the number of labelled records sharply declines at deeper taxonomic levels, especially beyond the family rank, which makes classification tasks more challenging.

4 Benchmark experiments and results

In real-world insect biodiversity monitoring, it is common to encounter both species which are already known to science, and samples whose species is novel. Thus, to excel in biodiversity monitoring, a model must correctly categorize instances of known species, and identify novel species outside the existing taxonomy, grouping together samples of the same new species. In our experiments, we explore three methods which offer utility in these regards, evaluated in two settings: closed-world and open-world. In the closed-world setting, the task is to accurately identify species from a predefined set of existing labels. In the open-world setting, the task is to group together samples of novel species.

4.1 Data partitioning

Species sets. We first partition records based on their species label into one of four categories, with all samples bearing the same species label being placed in the same species set. *Seen*: all samples whose species label is an established scientific name of a species. *Unseen*: labelled with an established scientific name for the genus, and a uniquely identifying placeholder name for the species. *Heldout*: labelled with a placeholder genus and species name. *Unknown*: samples without a species label (note: these may truly belong in any of the other three categories).

Table 3: Statistics and purpose of our data partitions.

Species set	Split	Purpose	N ^o Samples	N ^o Barcodes	N ^o Species
unknown seen	pretrain	SSL, semi-sup. training	4,677,756	2,284,232	—
	train	supervision; retrieval keys	289,203	118,051	11,846
	val	model dev; retrieval queries	14,757	6,588	3,378
	test	final eval; retrieval queries	39,373	18,362	3,483
unseen	key_unseen	retrieval keys	36,465	12,166	914
	val_unseen	model dev; retrieval queries	8,819	2,442	903
	test_unseen	final eval; retrieval queries	7,887	3,401	880
heldout	other_heldout	novelty detector training	76,590	41,250	9,862

Splits. Using the above species sets, we establish partitions for our experiments (Table 3). The *unknown* samples are all placed into a *pretrain* split for use in self-supervised pretraining and/or semi-supervised learning. As some DNA barcodes are common to multiple samples, for *seen* and *unseen* records we split the records by placing all samples with the same barcode in the same partition, to ensure there is no repetition of barcodes across splits. For the closed-world setting, we use the *seen* records to establish *train*, *val*, *test* splits. To ensure that the *test* set is not too imbalanced in species distribution, we place samples in the *test* set with a flattened distribution. We sample records from species with at least two unique barcodes and eight samples, and the number of samples placed in the *test* set scales linearly with the total number of samples for the species, until reaching a cap of 25 samples. We sample 5% of the remaining *seen* data to form the *val*, but in this case match the imbalance of the overall dataset. The remaining samples then form the *train* split, with a final split distribution of 84.2 : 4.3 : 11.5. Following standard practice, the *val* set is for model evaluation during development and hyperparameter tuning, and the *test* set is for final evaluation. In the retrieval setting, the *train* split should be used as a database of *keys* to retrieve over, and the *val* and *test* split as queries.

For the open-world scenario, we use a similar procedure to establish *val_unseen* and *test_unseen* over the *unseen* records. After creating *test_unseen* with the same methodology as *test*, we sample 20% of remaining *unseen* species records to create *val_unseen*. The remaining *unseen* species samples form the *keys_unseen* set. In the retrieval setting, *keys_unseen* is used to form the database of *keys* to retrieve, and the *val_unseen* and *test_unseen* splits act as queries. The *heldout* species samples form a final *other_heldout* partition. As these species are in neither *seen* nor *unseen*, this split can be used to train a novelty detector without using any *unseen* species.

4.2 DNA-based taxonomic classification

In this section, we discuss the utility of the BIOSCAN-5M dataset for DNA-based taxonomic classification. Due to their standardized length, DNA barcodes are ideal candidates as input to CNN- and transformer-based architectures for supervised taxonomic classification. However, as noted by Millan Arias et al. [52], a limitation of this approach is the uncertainty in species-level labels for a substantial portion of the data. This uncertainty, partly due to the lack of consensus among researchers and the continuous discovery of new species, may render supervised learning suboptimal for this task. We address this issue by adopting a semi-supervised learning approach. Specifically, we train a model using self-supervision on unlabelled sequences from the *pretrain* split and the *other_heldout* split, followed by fine-tuning on sequences from the *train* split, which includes high-quality labels. The same pretrained model can be used to produce embeddings for sequences from unseen taxa to address tasks in the open-world setting. Consequently, we use these embeddings to perform non-parametric taxonomic classification at a higher (less specific) level in the taxonomic hierarchy for evaluation.

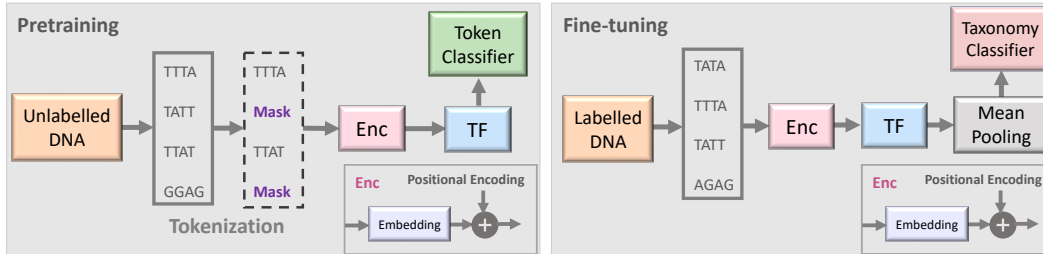


Figure 4: Two stages of the proposed semi-supervised learning set-up based on BarcodeBERT [52]. (1) Pretraining: DNA sequences are tokenized using non-overlapping k -mers and 50% of the tokens are masked for the MLM task. Tokens are encoded and fed into a transformer model. The output embeddings are used for token-level classification. (2) Fine-tuning: All DNA sequences in a dataset are tokenized using non-overlapping k -mer tokenization and all tokenized sequences, without masking, are passed through the pretrained transformer model. Global mean-pooling is applied over the token-level embeddings and the output is used for taxonomic classification.

Experimental setup. Although there has been a growing number of SSL DNA language models proposed in the recent literature, the results obtained by the recently proposed BarcodeBERT [52] model empirically demonstrate that training on a dataset of DNA barcodes can outperform more sophisticated training schemes that use a diverse set of non-barcode DNA sequences, such as DNABERT [38] and DNABERT-2 [85]. In this study, we selected BarcodeBERT as our reference model upon which to investigate the impact of pretraining on the larger and more diverse DNA barcode dataset BIOSCAN-5M. See Appendix A5 for pretraining details.

We compare our pretrained model against four pretrained transformer models: BarcodeBERT [52], DNABERT-2 [85], DNABERT-S [86], and the nucleotide transformer (NT) [14]; one state space model, HyenaDNA[56]; and a CNN baseline following the architecture introduced in [2].

As an additional assessment of the impact of BIOSCAN-5M DNA data during pretraining, we use the different pretrained models as feature extractors and evaluate the quality of the embeddings produced by the models on two different SSL evaluation strategies [4]. We first implement genus-level 1-NN probing on sequences from unseen species, providing insights into the models’ abilities to generalize to new taxonomic groups. Finally, we perform species-level classification using a linear classifier trained on embeddings from the pretrained models. Note that for both probing tasks, all the embeddings produced by a single sequence are averaged across the token dimension to generate a token embedding for the barcode.

Results. We leverage the different partitions of the data and make a distinction between the experiments in the closed-world and open-world settings. In the closed-world setting, the task is species-level identification of samples from species that have been seen during training (Fine-tuned accuracy, Linear probing accuracy). For reference, BLAST [1], an algorithmic sequence alignment tool, achieves an accuracy of 99.78% in the task (not included in Table 4 as it is not a machine learning model). In fine-tuning, our pretrained model with a 8-4-4 architecture achieves the highest accuracy with 99.28%, while DNABERT-2 achieves 99.23%, showing competitive performance. Overall, all models demonstrate strong performance in this task, showcasing the effectiveness of DNA barcodes in species-level identification. For linear probing accuracy, DNABERT-S outperforms others with 95.50%, followed by our model (8-4-4) with 94.47%. BarcodeBERT ($k=4$) and DNABERT-S also show strong performance with 91.93% and 91.59% respectively (see Table 4).

In the open-world setting, the task is to assign samples from unseen species to seen categories of a coarser taxonomic ranking (1NN-genus probing). In this task, BLAST achieves an accuracy of 58.74% (not in the table), and our model (8-4-4) performs notably well with an 47.03% accuracy, which is significantly higher than the other transformer models. The CNN baseline and HyenaDNA show lower accuracies of 29.88% and 19.26%, respectively. The use of DNA barcodes for pretraining in our models and BarcodeBERT demonstrates effectiveness in both seen and unseen species classification tasks. One limitation of the comparison is the difference in the dimension of the output space of the different models (128 for HyenaDNA, vs. 512 for NT and 768 for the BERT-based models). The selection of our model (8-4-4) as the best-performing configuration was done after performing a

Table 4: **Performance of DNA-based sequence models** in closed- and open-world settings. For the closed-world, we show the species-level accuracy (%) for predicting seen species (test), for open-world the genus-level accuracy (%) for test_unseen species while using seen species to fit the model. Bold indicates highest accuracy, underlined denotes second highest.

Model	Architecture	SSL-Pretraining	Tokens seen	Seen: Species		Unseen: Genus
				Fine-tuned	Linear probe	INN-Probe
CNN baseline	CNN	–	–	97.70	–	<u>29.88</u>
NT	Transformer	Multi-Species	300 B	98.99	52.41	21.67
DNABERT-2	Transformer	Multi-Species	512 B	99.23	67.81	17.99
DNABERT-S	Transformer	Multi-Species	~1,000 B	98.99	95.50	17.70
HyenaDNA	SSM	Human DNA	5 B	98.71	54.82	19.26
BarcodeBERT	Transformer	DNA barcodes	5 B	98.52	91.93	23.15
Ours (8-4-4)	Transformer	DNA barcodes	7 B	99.28	<u>94.47</u>	47.03

hyperparameter search to determine the optimal value of k for tokenization, as well as the optimal number of heads and layers in the transformer model. To do that, after pretraining, we fine-tuned the model for species-level identification and performed linear- and INN- probing on the validation split (see Table A15). We finally note that our pretrained model outperforms BarcodeBERT, the other model trained exclusively trained on DNA barcodes, across all tasks.

4.3 Zero-shot transfer-learning

Recent work has proposed the task of *zero-shot clustering*, investigating how well unseen datasets can be clustered using embeddings from pretrained feature extractors [47]. Lowe et al. [47] found that BIOSCAN-1M images were best clustered taxonomically at the family rank while retaining high clustering performance at species and BIN labels. We replicate this analysis using BIOSCAN-5M and extend the modality space to include both image and DNA barcodes.

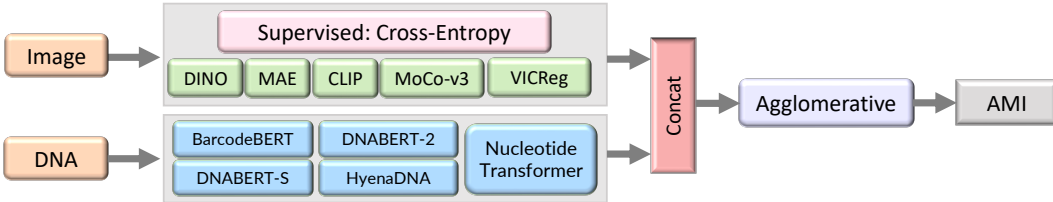


Figure 5: **Zero-shot clustering methodology.** Images and DNA are each passed through one of several pretrained encoders. These representations are clustered with Agglomerative Clustering.

Experimental setup. We follow the experimental setup recommended by Lowe et al. [47]. (1) Take pretrained encoders; (2) Extract feature vectors from the stimuli by passing them through an encoder; (3) Reduce dimensions to 50 using UMAP [51]; (4) Cluster the reduced embeddings with Agglomerative Clustering (L2, Ward’s method) [19]; (5) Evaluate against the ground-truth annotations with Adjusted Mutual Information (AMI) score [78].

For the image encoders, we consider ResNet-50 [27] and ViT-B [17] models, each pretrained on ImageNet-1K [64] using either supervised (Cross-entropy; X-ent.) or SSL methods (MAE [29], VICReg [5], DINO-v1 [11], MoCo-v3 [12]). We also considered the CLIP [61] encoder, which was pretrained on an unspecified, large dataset of captioned images. To cluster the DNA barcodes, we used several recent pretrained models described in §4.2 and §A5.2, which feature a variety of model architectures, pretraining datasets, and training methodologies: BarcodeBERT [52], DNABERT-2 [85], DNABERT-S [86], the nucleotide transformer (NT) [14], and HyenaDNA [56].

We only cluster samples from the test and test_unseen splits. None of the image or DNA pretraining datasets overlap with BIOSCAN-5M, so all samples are “unseen”. However, we note that there is a greater domain shift from the image pretraining datasets than the DNA pretraining datasets.

Results. Similar to Lowe et al. [47], we find (Figure 6) the clustered images best agreed with the taxonomic labels at the family rank, and the best-performing image encoder was DINO, followed

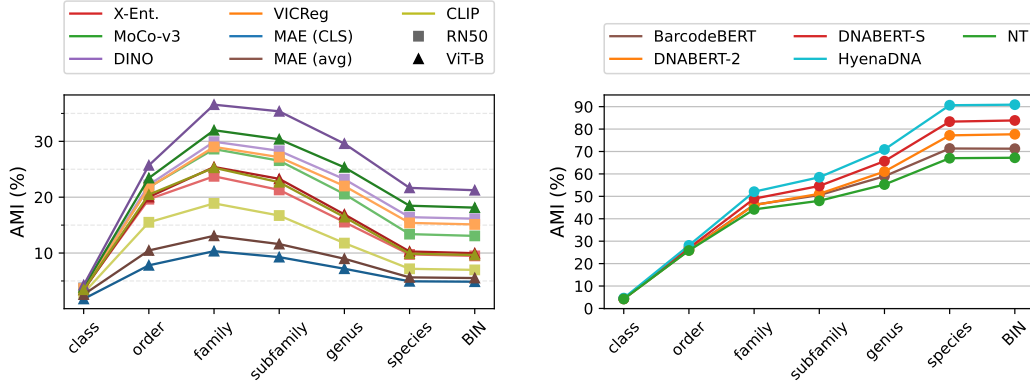


Figure 6: **Zero-shot clustering AMI (%) performance** across taxonomic ranks. Left: Image encoders. Right: DNA encoders.

by other SSL methods VICReg and MoCo-v3, with (larger) ViT-B models outperforming ResNet-50 models. The performance gradually declined when considering more fine-grained taxa. This difference from the findings of Lowe et al. [47] may be due to the flatter data balance compared with the BIOSCAN-1M splits. We found the performance of the DNA encoders exceeded that of the image encoders across all taxonomic levels, increasing monotonically as granularity becomes finer. HyenaDNA provided the best performance, with in excess of 90% agreement between its clusterings and the GT species and DNA BIN annotations. These results suggest that DNA barcodes are highly informative about species identity (which is unsurprising as it is the reason this barcode is used), and unseen samples can be readily grouped together using off-the-shelf DNA models.

We also considered the zero-shot clustering of the concatenated image and DNA representations, detailed in Appendix A6.3. Due to the high performance of the DNA features, adding image features to the embeddings decreased the performance compared to using DNA embeddings alone. For additional details and analysis, see Appendix A6.

4.4 Multimodal retrieval learning

Lastly, we demonstrate the importance of a multimodal dataset through alignment of image, DNA, and taxonomic label embeddings to improve taxonomic classification. By learning a shared embedding space across modalities, we can query between modalities and leverage the information across them to achieve better performance in downstream tasks. We are able to incorporate a diversity of samples into training toward taxonomic classification, even with incomplete taxonomic labels.

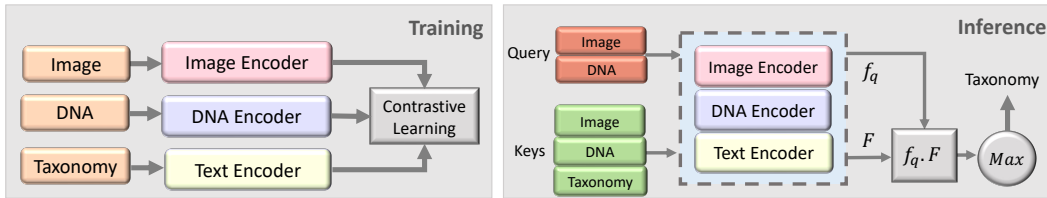


Figure 7: Our experiments using the BIOSCAN-CLIP [24] are conducted in two steps. (1) Training: Multiple modalities, including RGB images, textual taxonomy, and DNA sequences, are encoded separately, and trained using a contrastive loss function. (2) Inference: Image vs DNA embedding is used as a query, and compared to the embeddings obtained from a database of image, DNA and text (keys). The cosine similarity is used to find the closest key embedding, and the corresponding taxonomic label is used to classify the query.

Experimental setup. We follow the model architecture and experimental setup of Gong et al. [24]. We start with pretrained encoders for each modality and fine-tune them using LoRA [33] with NT-Xent loss [68]. Our image encoder is a ViT-B [17] pretrained on ImageNet-21k and fine-tuned on ImageNet-1k [15]. For DNA barcodes, we use BarcodeBERT [52] with 5-mer tokenization, pretrained on about 893 k DNA barcodes, and for text, we use BERT-small [74]. We train on the pretrain and

Table 5: Top-1 macro accuracy (%) on the test set for using different pre-train datasets (BIOSCAN-1M, BIOSCAN-5M) and different combinations of aligned embeddings (image, DNA, text) during contrastive training. We show results for using image-to-image, DNA-to-DNA, and image-to-DNA query and key combinations. As a baseline, we show the results prior to contrastive learning (no alignment). We report the accuracy for seen and unseen species, and the harmonic mean (H.M.) between these (bold: highest acc.).

Taxon	Trained on	Aligned embeddings			DNA to DNA			Image to Image			Image to DNA		
		Img	DNA	Txt	Seen	Unseen	H.M.	Seen	Unseen	H.M.	Seen	Unseen	H.M.
Order	—	×	×	×	95.8	97.8	96.8	78.1	82.4	80.2	3.6	6.3	4.6
	BS-1M	✓	✓	✓	99.2	100.0	99.6	88.9	89.0	89.0	32.5	51.9	40.0
	BS-5M	✓	✓	×	96.1	99.9	98.0	90.2	94.0	92.1	65.4	90.6	76.0
	BS-5M	✓	✓	✓	98.9	100.0	99.4	93.5	91.3	92.4	68.1	94.6	79.2
Family	—	×	×	×	90.2	92.1	91.2	52.3	55.5	53.8	0.3	1.0	0.4
	BS-1M	✓	✓	✓	95.5	96.9	96.2	73.9	75.0	74.4	21.4	43.1	28.6
	BS-5M	✓	✓	×	90.3	93.2	91.8	74.8	78.3	76.5	30.4	50.5	38.0
	BS-5M	✓	✓	✓	94.9	97.6	96.2	75.3	77.8	76.5	31.2	54.2	39.6
Genus	—	×	×	×	86.8	85.7	86.2	34.0	31.9	32.9	0.0	0.0	0.0
	BS-1M	✓	✓	✓	89.8	85.7	87.7	58.4	58.1	58.2	9.5	15.6	11.8
	BS-5M	✓	✓	×	79.5	72.9	76.1	58.4	59.8	59.1	13.7	16.8	15.1
	BS-5M	✓	✓	✓	87.8	84.4	86.1	58.6	58.3	58.5	13.8	17.3	15.4
Species	—	×	×	×	84.6	75.6	79.8	24.2	12.6	16.6	0.0	0.0	0.0
	BS-1M	✓	✓	✓	85.5	62.8	72.4	46.5	31.4	37.5	5.3	2.5	3.4
	BS-5M	✓	✓	×	74.0	43.7	55.0	46.4	31.1	37.2	8.4	2.4	3.7
	BS-5M	✓	✓	✓	83.0	59.0	69.0	46.1	29.1	35.7	7.5	2.2	3.4

train splits using the Adam [42] optimizer for 4 epochs until convergence with a learning rate of 0.001 and batch size of 800. Training took roughly 52 hours on two 80GB A100 GPUs. To evaluate the performance of our models, we report micro (see Appendix A7) and macro top-1 accuracy for taxonomic classification for order, family, genus, and species. To determine the taxonomic labels for a new query, we encode the sample image or DNA and find the closest matching embedding in a dataset of labeled samples (keys). For efficient lookup, we use the FAISS [39] library with exact search (IndexFlatIP). We compare using image-to-image, DNA-to-DNA, and image-to-DNA embeddings as the queries and keys, respectively.

Results. We compare BIOSCAN-CLIP trained on BIOSCAN-5M against models trained on BIOSCAN-1M and models using frozen encoders (no contrastive training). Our result in Table 5 shows that that our model improves classification accuracy for same-modality queries and enables cross-modality queries. By aligning to DNA, our image embeddings are able to capture finer details, while aligning to image embeddings causes the DNA embeddings to be a bit less precise at the genera and species level. Additionally, the increased dataset size of BIOSCAN-5M for these taxa leads to better models with more accurate results. However, performance is more varied at the species level, suggesting the difficulty of prediction at the most fine-grained level. Similar observations are made when using images only. For DNA querying and retrieval, we see the fewest patterns of improvement from the BIOSCAN-5M model, possibly resulting from the strength of the pretrained BarcodeBERT encoder, such that few improvements are seen through contrastive training for the DNA space specifically. For additional details and analysis, see Appendix A7.

5 Conclusion

We have introduced to the machine learning community a valuable resource: the BIOSCAN-5M dataset, containing over 5 million arthropod specimens. To showcase the multi-modal features of this dataset, we conducted three benchmark experiments. These combine images, DNA barcodes, and textual taxonomic annotations for fine-grained taxonomic classification and zero-shot clustering.

We hope that the BIOSCAN-5M dataset will serve as a catalyst for further machine learning research in biodiversity, fostering innovations that can enhance our understanding and preservation of the natural world. By providing a curated multi-modal resource, we aim to support further initiatives in the spirit of TreeOfLife-10M [72] and contribute to the broader goal of mapping and preserving global biodiversity. This dataset not only facilitates advanced computational approaches but also

underscores the crucial intersection between technology and conservation science, driving forward efforts to protect our planet's diverse ecosystems for future generations.

Acknowledgement

We acknowledge the support of the Government of Canada’s New Frontiers in Research Fund (NFRF), [NFRFT-2020-00073]. Nous remercions le fonds Nouvelles frontières en recherche du gouvernement du Canada de son soutien [FNFRF-2020-00073]. This research is also supported by an NVIDIA Academic Grant. This research was enabled in part by support provided by Calcul Québec* and the Digital Research Alliance of Canada*. Resources used in preparing this research were provided, in part, by the Province of Ontario, the Government of Canada through CIFAR, and companies sponsoring* the Vector Institute. Data collection was enabled by funds from the Walder Foundation, a New Frontiers in Research Fund (NFRF) Transformation grant, a Canada Foundation for Innovation’s (CFI) Major Science Initiatives (MSI) Fund and CFREF funds to the Food from Thought program at the University of Guelph. The authors also wish to acknowledge the team at the Centre for Biodiversity Genomics responsible for preparing, imaging, and sequencing specimens used for this study. We also thank Mrinal Goshalia for assistance with the cropping tool and annotation of images.

References

- [1] Altschul, S. F., Gish, W., Miller, W., Myers, E. W., and Lipman, D. J. Basic local alignment search tool. *Journal of Molecular Biology*, 215(3):403–410, 1990. ISSN 0022-2836. doi:10.1016/S0022-2836(05)80360-2.
- [2] Badirli, S., Akata, Z., Mohler, G., Picard, C., and Dundar, M. Fine-grained zero-shot learning with DNA as side information. In *Advances in Neural Information Processing Systems 34 (NeurIPS 2021)*, December 2021.
- [3] Badirli, S., Picard, C. J., Mohler, G., Richert, F., Akata, Z., and Dundar, M. Classifying the unknown: Insect identification with deep hierarchical Bayesian learning. *Methods in Ecology and Evolution*, 14(6):1515–1530, 2023.
- [4] Balestrieri, R., Ibrahim, M., Sobal, V., Morcos, A., Shekhar, S., Goldstein, T., Bordes, F., Bardes, A., Mialon, G., Tian, Y., et al. A cookbook of self-supervised learning. *arXiv preprint arXiv:2304.12210*, 2023. doi:10.48550/arxiv.2304.12210.
- [5] Bardes, A., Ponce, J., and LeCun, Y. VICReg: Variance-invariance-covariance regularization for self-supervised learning. *arXiv preprint arXiv:2105.04906*, 2021. doi:10.48550/arxiv.2105.04906.
- [6] Blaxter, M., Mann, J., Chapman, T., Thomas, F., Whitton, C., Floyd, R., and Abebe, E. Defining operational taxonomic units using DNA barcode data. *Philosophical Transactions of the Royal Society B: Biological Sciences*, 360(1462):1935–1943, 2005.
- [7] Braukmann, T. W., Ivanova, N. V., Prosser, S. W., Elbrecht, V., Steinke, D., Ratnasingham, S., de Waard, J. R., Sones, J. E., Zakharov, E. V., and Hebert, P. D. Metabarcoding a diverse arthropod mock community. *Molecular ecology resources*, 19(3):711–727, 2019.
- [8] Brown, T., Mann, B., Ryder, N., Subbiah, M., Kaplan, J. D., Dhariwal, P., Neelakantan, A., Shyam, P., Sastry, G., Askell, A., et al. Language models are few-shot learners. *Advances in neural information processing systems*, 33:1877–1901, 2020.
- [9] Cardinale, B. J., Duffy, J. E., Gonzalez, A., Hooper, D. U., Perrings, C., Venail, P., Narwani, A., Mace, G. M., Tilman, D., Wardle, D. A., et al. Biodiversity loss and its impact on humanity. *Nature*, 486(7401):59–67, 2012.
- [10] Carion, N., Massa, F., Synnaeve, G., Usunier, N., Kirillov, A., and Zagoruyko, S. End-to-end object detection with transformers. In *Proc. of the European Conference on Computer Vision*, pp. 213–229. Springer, 2020.

*<https://calculquebec.ca>

*<https://alliancecan.ca>

*<https://vectorinstitute.ai/partnerships/current-partners/>

- [11] Caron, M., Touvron, H., Misra, I., Jégou, H., Mairal, J., Bojanowski, P., and Joulin, A. Emerging properties in self-supervised vision transformers. In *Proceedings of the International Conference on Computer Vision (ICCV)*, 2021.
- [12] Chen, X., Xie, S., and He, K. An empirical study of training self-supervised vision transformers. *arXiv preprint arXiv:2104.02057*, 2021. doi:10.48550/arxiv.2104.02057.
- [13] Chia, P. J., Attanasio, G., Bianchi, F., Terragni, S., Magalhães, A. R., Goncalves, D., Greco, C., and Tagliabue, J. Contrastive language and vision learning of general fashion concepts. *Scientific Reports*, 12(1):18958, 2022.
- [14] Dalla-Torre, H., Gonzalez, L., Mendoza-Revilla, J., Carranza, N. L., Grzywaczewski, A. H., Oteri, F., Dallago, C., Trop, E., de Almeida, B. P., Sirelkhatim, H., et al. The nucleotide transformer: Building and evaluating robust foundation models for human genomics. *bioRxiv*, pp. 2023–01, 2023.
- [15] Deng, J., Dong, W., Socher, R., Li, L.-J., Li, K., and Fei-Fei, L. ImageNet: A large-scale hierarchical image database. In *2009 IEEE conference on computer vision and pattern recognition*, pp. 248–255. Ieee, 2009.
- [16] Dosovitskiy, A., Beyer, L., Kolesnikov, A., Weissenborn, D., Zhai, X., Unterthiner, T., Dehghani, M., Minderer, M., Heigold, G., Gelly, S., et al. An image is worth 16x16 words: Transformers for image recognition at scale. *arXiv preprint arXiv:2010.11929*, 2020. doi:10.48550/arxiv.2010.11929.
- [17] Dosovitskiy, A., Beyer, L., Kolesnikov, A., Weissenborn, D., Zhai, X., Unterthiner, T., Dehghani, M., Minderer, M., Heigold, G., Gelly, S., Uszkoreit, J., and Houlsby, N. An image is worth 16x16 words: Transformers for image recognition at scale. In *9th International Conference on Learning Representations*, 2021. URL <https://openreview.net/forum?id=YicbFdNTTy>.
- [18] Duraiappah, A. K., Naeem, S., Agardy, T., Ash, N. J., Cooper, H. D., Díaz, S., Faith, D. P., Mace, G., McNeely, J. A., Mooney, H. A., et al. Ecosystems and human well-being: biodiversity synthesis; a report of the Millennium Ecosystem Assessment. Technical report, World Resources Institute, 2005.
- [19] Everitt, B. S., Landau, S., Leese, M., and Stahl, D. *Cluster Analysis*. Wiley, January 2011. doi:10.1002/9780470977811.
- [20] Flicek, P., Amode, M., Barrell, D., Beal, K., Billis, K., Brent, S., Carvalho-Silva, D., Clapham, P., Coates, G., Fitzgerald, S., Gil, L., Girón, C., Gordon, L., et al. Ensembl 2014. *Nucleic Acids Res.*, 42:D749–55, 2014.
- [21] Galloway, A., Taylor, G. W., Ramsay, A., and Moussa, M. The Ciona17 dataset for semantic segmentation of invasive species in a marine aquaculture environment. In *2017 14th Conference on Computer and Robot Vision (CRV)*, pp. 361–366. IEEE, 2017. doi:10.1109/CRV.2017.46.
- [22] Garcin, C., Joly, A., Bonnet, P., Lombardo, J.-C., Affouard, A., Chouet, M., Servajean, M., Lorieul, T., and Salmon, J. Pl@ntNet-300K: a plant image dataset with high label ambiguity and a long-tailed distribution. In *NeurIPS 2021-35th Conference on Neural Information Processing Systems*, 2021.
- [23] Gharaee, Z., Gong, Z., Pellegrino, N., Zarubiieva, I., Haurum, J. B., Lowe, S. C., McKeown, J. T. A., Ho, C. C. Y., McLeod, J., Wei, Y.-Y. C., Agda, J., Ratnasingham, S., Steinke, D., Chang, A. X., Taylor, G. W., and Fieguth, P. A step towards worldwide biodiversity assessment: The BIOSCAN-1M insect dataset. In Oh, A., Neumann, T., Globerson, A., Saenko, K., Hardt, M., and Levine, S. (eds.), *Advances in Neural Information Processing Systems*, volume 36, pp. 43593–43619. Curran Associates, Inc., 2023. URL https://proceedings.neurips.cc/paper_files/paper/2023/file/87dbbdc3a685a97ad28489a1d57c45c1-Paper-Datasets_and_Benchmarks.pdf.
- [24] Gong, Z., Wang, A. T., Haurum, J. B., Lowe, S. C., Taylor, G. W., and Chang, A. X. BIOSCAN-CLIP: Bridging vision and genomics for biodiversity monitoring at scale. *arXiv preprint arXiv:2405.17537*, 2024. doi:10.48550/arxiv.2405.17537.

- [25] Goyal, P., Caron, M., Lefaudeux, B., Xu, M., Wang, P., Pai, V., Singh, M., Liptchinsky, V., Misra, I., Joulin, A., et al. Self-supervised pretraining of visual features in the wild. *arXiv preprint arXiv:2103.01988*, 2021. doi:10.48550/arxiv.2103.01988.
- [26] Gu, Y., Tinn, R., Cheng, H., Lucas, M., Usuyama, N., Liu, X., Naumann, T., Gao, J., and Poon, H. Domain-specific language model pretraining for biomedical natural language processing. *ACM Transactions on Computing for Healthcare (HEALTH)*, 3(1):1–23, 2021.
- [27] He, K., Zhang, X., Ren, S., and Sun, J. Deep residual learning for image recognition. In *2016 IEEE Conference on Computer Vision and Pattern Recognition (CVPR)*, pp. 770–778, 2016. doi:10.1109/CVPR.2016.90.
- [28] He, K., Zhang, X., Ren, S., and Sun, J. Deep residual learning for image recognition. In *Proceedings of the IEEE conference on computer vision and pattern recognition*, pp. 770–778, 2016.
- [29] He, K., Chen, X., Xie, S., Li, Y., Dollár, P., and Girshick, R. Masked autoencoders are scalable vision learners. In *Proceedings of the IEEE/CVF conference on computer vision and pattern recognition*, pp. 16000–16009, 2022.
- [30] He, W., Han, K., Nie, Y., Wang, C., and Wang, Y. Species196: A one-million semi-supervised dataset for fine-grained species recognition. *Advances in Neural Information Processing Systems*, 36, 2024.
- [31] Hebert, P. D., Cywinska, A., Ball, S. L., and DeWaard, J. R. Biological identifications through DNA barcodes. *Proceedings of the Royal Society of London. Series B: Biological Sciences*, 270(1512):313–321, 2003.
- [32] Hickling, R., Roy, D. B., Hill, J. K., Fox, R., and Thomas, C. D. The distributions of a wide range of taxonomic groups are expanding polewards. *Global change biology*, 12(3):450–455, 2006.
- [33] Hu, E. J., Shen, Y., Wallis, P., Allen-Zhu, Z., Li, Y., Wang, S., Wang, L., and Chen, W. LoRA: Low-rank adaptation of large language models. In *International Conference on Learning Representations*, 2022. URL <https://openreview.net/forum?id=nZeVKeeFYf9>.
- [34] Ikezogwo, W., Seyfioglu, S., Ghezloo, F., Geva, D., Sheikh Mohammed, F., Anand, P. K., Krishna, R., and Shapiro, L. Quilt-1M: One million image-text pairs for histopathology. *Advances in Neural Information Processing Systems*, 36, 2024.
- [35] Ilyas, T., Arsa, D. M. S., Ahmad, K., Jeong, Y. C., Won, O., Lee, J. H., and Kim, H. CWD30: A comprehensive and holistic dataset for crop weed recognition in precision agriculture. *arXiv preprint arXiv:2305.10084*, 2023. doi:10.48550/arxiv.2305.10084.
- [36] International Barcode of Life Consortium. Barcode of Life Data System. URL <https://boldsystems.org/>.
- [37] Jensen, P. B., Jensen, L. J., and Brunak, S. Mining electronic health records: towards better research applications and clinical care. *Nature Reviews Genetics*, 13:395–405, 2012.
- [38] Ji, Y., Zhou, Z., Liu, H., and Davuluri, R. V. DNABERT: pre-trained bidirectional encoder representations from transformers model for DNA-language in genome. *Bioinformatics*, 37(15): 2112–2120, 2021.
- [39] Johnson, J., Douze, M., and Jégou, H. Billion-scale similarity search with GPUs. *IEEE Transactions on Big Data*, 7(3):535–547, 2019.
- [40] Kattge, J., Diaz, S., Lavorel, S., Prentice, I. C., Leadley, P., Bonisch, G., Garnier, E., Westoby, M., Reich, P. B., Wright, I. J., Cornelissen, J. H. C., Violle, C., Harrison, S. P., et al. TRY – a global database of plant traits. *Global Change Biology*, 17(9):2905–2935, 2011.
- [41] Kim, M.-S., Pinto, S. M., Getnet, D., Nirujogi, R. S., Manda, S. S., Chaerkady, R., Madugundu, A. K., et al. A draft map of the human proteome. *Nature*, 509:575–581, 2014.

- [42] Kingma, D. P. and Ba, J. Adam: A method for stochastic optimization. *arXiv preprint arXiv:1412.6980*, 2014. doi:10.48550/arxiv.1412.6980.
- [43] Kumar, N., Belhumeur, P. N., Biswas, A., Jacobs, D. W., Kress, W. J., Lopez, I. C., and Soares, J. V. Leafsnap: A computer vision system for automatic plant species identification. In *Computer Vision—ECCV 2012: 12th European Conference on Computer Vision, Florence, Italy, October 7–13, 2012, Proceedings, Part II 12*, pp. 502–516. Springer, 2012.
- [44] Lin, T.-Y., Maire, M., Belongie, S., Hays, J., Perona, P., Ramanan, D., Dollár, P., and Zitnick, C. L. Microsoft COCO: Common objects in context. In *Proc. of the European Conference on Computer Vision*, pp. 740–755. Springer, 2014.
- [45] Liu, X., Min, W., Mei, S., Wang, L., and Jiang, S. Plant disease recognition: A large-scale benchmark dataset and a visual region and loss reweighting approach. *IEEE Trans Image Process*, 30:2003–2015, 2021.
- [46] Loshchilov, I. and Hutter, F. Decoupled weight decay regularization. In *International Conference on Learning Representations (ICLR)*, 2019. doi:10.48550/arxiv.1711.05101. URL <https://openreview.net/forum?id=Bkg6RiCqY7>.
- [47] Lowe, S. C., Haurum, J. B., Oore, S., Moeslund, T. B., and Taylor, G. W. An empirical study into clustering of unseen datasets with self-supervised encoders. *arXiv preprint arXiv:2406.02465*, 2024. doi:10.48550/arxiv.2406.02465.
- [48] Lowe, S. C., Misiuk, B., Xu, I., Abdulazizov, S., Baroi, A. R., Bastos, A. C., Best, M., Ferrini, V., Friedman, A., Hart, D., Hoegh-Guldberg, O., Ierodiaconou, D., Mackin-McLaughlin, J., Markey, K., Menandro, P. S., Monk, J., Nemani, S., O’Brien, J., Oh, E., Reshitnyk, L. Y., Robert, K., Roelfsema, C. M., Sameoto, J. A., Schimel, A. C. G., Thomson, J. A., Wilson, B. R., Wong, M. C., Brown, C. J., and Trappenberg, T. BenthicNet: A global compilation of seafloor images for deep learning applications. *arXiv preprint arXiv:2405.05241*, 2024. doi:10.48550/arxiv.2405.05241.
- [49] Lu, M. Y., Chen, B., Williamson, D. F., Chen, R. J., Liang, I., Ding, T., Jaume, G., Odintsov, I., Zhang, A., Le, L. P., et al. Towards a visual-language foundation model for computational pathology. *arXiv preprint arXiv:2307.12914*, 2023. doi:10.48550/arxiv.2307.12914.
- [50] Lu, Y. and Young, S. A survey of public datasets for computer vision tasks in precision agriculture. *Computers and Electronics in Agriculture*, 178:105760, 2020.
- [51] McInnes, L., Healy, J., and Melville, J. UMAP: Uniform manifold approximation and projection for dimension reduction. *arXiv preprint arXiv:1802.03426*, 2018. doi:10.48550/arxiv.1802.03426.
- [52] Millan Arias, P., Sadjadi, N., Safari, M., Gong, Z., Wang, A. T., Lowe, S. C., Bruslund Haurum, J., Zarubiieva, I., Steinke, D., Kari, L., et al. BarcodeBERT: Transformers for biodiversity analysis. *arXiv preprint arXiv:2405.17537*, 2023. doi:10.48550/arxiv.2405.17537.
- [53] Mock, F., Kretschmer, F., Kriese, A., Böcker, S., and Marz, M. Taxonomic classification of DNA sequences beyond sequence similarity using deep neural networks. *Proceedings of the National Academy of Sciences*, 119(35):e2122636119, 2022.
- [54] Moritz, C. and Cicero, C. DNA barcoding: promise and pitfalls. *PLoS biology*, 2(10):e354, 2004.
- [55] Network, C. G. A. R., Weinstein, J., Collisson, E., Mills, G., Shaw, K., Ozenberger, B., Ellrott, K., Shmulevich, I., Sander, C., and Stuart, J. The cancer genome atlas pan-cancer analysis project. *Nat Genet.*, 45:1113–20, 2013.
- [56] Nguyen, E., Poli, M., Faizi, M., Thomas, A., Wornow, M., Birch-Sykes, C., Massaroli, S., Patel, A., Rabideau, C., Bengio, Y., et al. HyenaDNA: Long-range genomic sequence modeling at single nucleotide resolution. *Advances in neural information processing systems*, 36, 2024.

- [57] Nguyen, H.-Q., Truong, T.-D., Nguyen, X.-B., Downling, A., Li, X., and Luu, K. Insect-Foundation: A foundation model and large-scale 1M dataset for visual insect understanding. In *Proceedings of the IEEE/CVF Conference on Computer Vision and Pattern Recognition (CVPR)*, June 2024.
- [58] Olsen, A., Konovalov, D. A., Philippa, B., Ridd, P., Wood, J. C., Johns, J., Banks, W., Girgenti, B., Kenny, O., Whinney, J., et al. DeepWeeds: A multiclass weed species image dataset for deep learning. *Scientific reports*, 9(1):2058, 2019.
- [59] Pawlowski, J., Kelly-Quinn, M., Altermatt, F., Apothéloz-Perret-Gentil, L., Beja, P., Boggero, A., Borja, A., Bouchez, A., Cordier, T., Domaizon, I., et al. The future of biotic indices in the ecogenomic era: Integrating (e)DNA metabarcoding in biological assessment of aquatic ecosystems. *Science of the Total Environment*, 637:1295–1310, 2018.
- [60] Poli, M., Massaroli, S., Nguyen, E., Fu, D. Y., Dao, T., Baccus, S., Bengio, Y., Ermon, S., and Ré, C. Hyena hierarchy: Towards larger convolutional language models. In *International Conference on Machine Learning*, pp. 28043–28078. PMLR, 2023.
- [61] Radford, A., Kim, J. W., Hallacy, C., Ramesh, A., Goh, G., Agarwal, S., Sastry, G., Askell, A., Mishkin, P., Clark, J., et al. Learning transferable visual models from natural language supervision. In *International conference on machine learning*, pp. 8748–8763. PMLR, 2021.
- [62] Ratnasingham, S. and Hebert, P. D. A DNA-based registry for all animal species: the Barcode Index Number (BIN) system. *PloS one*, 8(7):e66213, 2013.
- [63] Ruppert, K. M., Kline, R. J., and Rahman, M. S. Past, present, and future perspectives of environmental DNA (eDNA) metabarcoding: A systematic review in methods, monitoring, and applications of global eDNA. *Global Ecology and Conservation*, 17:e00547, 2019.
- [64] Russakovsky, O., Deng, J., Su, H., Krause, J., Satheesh, S., Ma, S., Huang, Z., Karpathy, A., Khosla, A., Bernstein, M., Berg, A. C., and Fei-Fei, L. ImageNet large scale visual recognition challenge. *International Journal of Computer Vision*, 115(3):211–252, April 2015. doi:10.1007/s11263-015-0816-y.
- [65] Sala, O. E., Stuart Chapin, F., Armesto, J. J., Berlow, E., Bloomfield, J., Dirzo, R., Huber-Sanwald, E., Huenneke, L. F., Jackson, R. B., Kinzig, A., et al. Global biodiversity scenarios for the year 2100. *science*, 287(5459):1770–1774, 2000.
- [66] Sheridan, J. A. and Bickford, D. Shrinking body size as an ecological response to climate change. *Nature climate change*, 1(8):401–406, 2011.
- [67] Smith, L. N. and Topin, N. Super-convergence: Very fast training of residual networks using large learning rates. *arXiv preprint*, arXiv:1708.07120, 2017. doi:10.48550/arxiv.1708.07120.
- [68] Sohn, K. Improved deep metric learning with multi-class n-pair loss objective. In Lee, D., Sugiyama, M., Luxburg, U., Guyon, I., and Garnett, R. (eds.), *Advances in Neural Information Processing Systems*, volume 29. Curran Associates, Inc., 2016. URL https://proceedings.neurips.cc/paper_files/paper/2016/file/6b180037abbebea991d8b1232f8a8ca9-Paper.pdf.
- [69] Sokal, R. and Sneath, P. *Principles of Numerical Taxonomy*. Series of books in biology. W. H. Freeman, 1963.
- [70] Steckel, R. H. Stature and the standard of living. *Journal of economic literature*, 33(4): 1903–1940, 1995.
- [71] Steinke, D., Ratnasingham, S., Agda, J., Ait Boutou, H., Box, I., Chan, D., Doyle, M., Feng, C., McKeown, J., McLeod, J., Sanchez, A., Smith, I., Walker, S., Wei, C., and Hebert, P. Capturing biodiversity through the lens – 5.6 million arthropod images. *bioRxiv*, 2024.
- [72] Stevens, S., Wu, J., Thompson, M. J., Campolongo, E. G., Song, C. H., Carlyn, D. E., Dong, L., Dahdul, W. M., Stewart, C., Berger-Wolf, T., et al. BioCLIP: A vision foundation model for the tree of life. *arXiv preprint arXiv:2311.18803*, 2023. doi:10.48550/arxiv.2311.18803.

- [73] Stoeck, T., Frühe, L., Forster, D., Cordier, T., Martins, C. I., and Pawlowski, J. Environmental DNA metabarcoding of benthic bacterial communities indicates the benthic footprint of salmon aquaculture. *Marine Pollution Bulletin*, 127:139–149, 2018.
- [74] Turc, I., Chang, M.-W., Lee, K., and Toutanova, K. Well-read students learn better: On the importance of pre-training compact models. *arXiv preprint arXiv:1908.08962*, 2019. doi:10.48550/arxiv.1908.08962.
- [75] Van Horn, G., Branson, S., Farrell, R., Haber, S., Barry, J., Ipeirotis, P., Perona, P., and Belongie, S. Building a bird recognition app and large scale dataset with citizen scientists: The fine print in fine-grained dataset collection. In *Proceedings of the IEEE Conference on Computer Vision and Pattern Recognition*, pp. 595–604, 2015.
- [76] Van Horn, G., Cole, E., Beery, S., Wilber, K., Belongie, S., and Mac Aodha, O. Benchmarking representation learning for natural world image collections. In *Proceedings of the IEEE/CVF conference on computer vision and pattern recognition*, pp. 12884–12893, 2021.
- [77] Vaze, S., Han, K., Vedaldi, A., and Zisserman, A. Generalized category discovery. In *Proceedings of the IEEE/CVF Conference on Computer Vision and Pattern Recognition*, pp. 7492–7501, 2022.
- [78] Vinh, N. X., Epps, J., and Bailey, J. Information theoretic measures for clusterings comparison: Variants, properties, normalization and correction for chance. *Journal of Machine Learning Research*, 11(95):2837–2854, 2010. URL <http://jmlr.org/papers/v11/vinh10a.html>.
- [79] Wang, Q.-J., Zhang, S.-Y., Dong, S.-F., Zhang, G.-C., Yang, J., Li, R., and Wang, H.-Q. Pest24: A large-scale very small object data set of agricultural pests for multi-target detection. *Computers and Electronics in Agriculture*, 175:105585, 2020.
- [80] Wegner, J. D., Branson, S., Hall, D., Schindler, K., and Perona, P. Cataloging public objects using aerial and street-level images-urban trees. In *Proceedings of the IEEE Conference on Computer Vision and Pattern Recognition*, pp. 6014–6023, 2016.
- [81] Wu, X., Zhan, C., Lai, Y.-K., Cheng, M.-M., and Yang, J. IP102: A large-scale benchmark dataset for insect pest recognition. In *Proceedings of the IEEE/CVF conference on computer vision and pattern recognition*, pp. 8787–8796, 2019.
- [82] Xu, D., Zhao, Y., Hao, X., and Meng, X. Pink-Eggs Dataset V1: A step toward invasive species management using deep learning embedded solutions. *arXiv preprint arXiv:2305.09302*, 2023. doi:10.48550/arxiv.2305.09302.
- [83] Zhang, S., Xu, Y., Usuyama, N., Xu, H., Bagga, J., Tinn, R., Preston, S., Rao, R., Wei, M., Valluri, N., et al. BiomedCLIP: a multimodal biomedical foundation model pretrained from fifteen million scientific image-text pairs. *arXiv preprint arXiv:2303.00915*, 2023. doi:10.48550/arxiv.2303.00915.
- [84] Zhou, X. and Zhang, N. L. Deep clustering with features from self-supervised pretraining. *arXiv preprint arXiv:2207.13364*, 2022. doi:10.48550/arxiv.2207.13364.
- [85] Zhou, Z., Ji, Y., Li, W., Dutta, P., Davuluri, R., and Liu, H. DNABERT-2: Efficient foundation model and benchmark for multi-species genome. *arXiv preprint arXiv:2306.15006*, 2023. doi:10.48550/arxiv.2306.15006.
- [86] Zhou, Z., Wu, W., Ho, H., Wang, J., Shi, L., Davuluri, R. V., Wang, Z., and Liu, H. DNABERT-S: Learning species-aware DNA embedding with genome foundation models. *arXiv preprint arXiv:2402.08777*, 2024. doi:10.48550/arxiv.2402.08777.

Appendix

A1 Dataset

A1.1 Ethics and responsible use

The BIOSCAN project was instigated by the International Barcode of Life (iBOL) Consortium, which has collected a large dataset of manually-labelled images of organisms [36, 71]. As part of our project, we conducted a thorough review to identify any potential ethical issues related to the inclusion of our data sources. After careful evaluation, we did not find any ethical concerns. Therefore, we confirm that this work adheres to all relevant ethical standards and guidelines.

A1.2 Dataset availability and maintenance

There will be a landing page for publishing the dataset as well as a Google Drive folder to upload all dataset packages and other files related to the paper.

The BIOSCAN dataset and all its contents are available in Google Drive. To obtain the BIOSCAN dataset, please visit <https://biodiversitygenomics.net/5M-insects/>. We also release a code repository to manipulate the dataset, which handles multiple tasks including reading images and metadata, cropping images, splitting the dataset to train, validation, and test sets, and also running benchmark experiments presented in the BIOSCAN-5M paper. To access the BIOSCAN-5M code repository, please visit <https://github.com/zahrag/BIOSCAN-5M>.

A1.3 Licensing

Table A1 shows all the copyright associations related to the BIOSCAN-5M dataset with the corresponding names and contact information.

Table A1: Copyright associations related to the BIOSCAN-5M dataset

Copyright Associations	Name & Contact
Image Photographer	CBG Robotic Imager
Copyright Holder	CBG Photography Group
Copyright Institution	Centre for Biodiversity Genomics (email: CBGImaging@gmail.com)
Copyright License	Creative Commons Attribution 3.0 Unported (CC BY 3.0)
Copyright Contact	collectionsBIO@gmail.com
Copyright Year	2021

The authors state that they bear all responsibility in case of violation of usage rights.

A1.4 RGB images

The BIOSCAN-5M dataset comprises resized and cropped images, as introduced in BIOSCAN-1M Insect [23]. We have provided various packages of the BIOSCAN-5M dataset, detailed in Table A2, each tailored for specific purposes.

- `original_full`: The raw images of the dataset, typically 1024×768 pixels.
- `cropped`: Images after cropping with our cropping tool (see §A4.1).
- `original_256`: Original images resized to 256 on their shorter side (most 341×256 pixels).
- `cropped_256`: Cropped images resized to 256 on their shorter side.

Among these, the `original_256` and `cropped_256` packages are specifically provided for experimentation as they are small and easy to work with. Therefore, using our predefined split partitions, we provide per-split experimental packages in addition to the packages with all the `original_256` and `cropped_256` images.

Accessing the dataset images is facilitated by the following directory structure used to organize the dataset images:

Table A2: Various downloadable packages of the images comprising the BIOSCAN-5M dataset.

Image set	Package	Partition(s)	Size (GB)	N ^o Parts
original_full	BIOSCAN_5M_original_full.zip	All	200	5
cropped	BIOSCAN_5M_cropped.zip	All	77.2	2
original_256	BIOSCAN_5M_original_256.zip	All	35.2	1
	BIOSCAN_5M_original_256_pretrain.zip	Pretrain	31.7	1
	BIOSCAN_5M_original_256_train.zip	Train	2.1	1
	BIOSCAN_5M_original_256_eval.zip	Evaluation	1.4	1
cropped_256	BIOSCAN_5M_cropped_256.zip	All	36.4	1
	BIOSCAN_5M_cropped_256_pretrain.zip	Pretrain	33.0	1
	BIOSCAN_5M_cropped_256_train.zip	Train	2.1	1
	BIOSCAN_5M_cropped_256_eval.zip	Evaluation	1.4	1

`bioscan5m/images/[imgtype]/[split]/[chunk]/[processid].jpg`

where `[imgtype]` can be `original_full`, `cropped`, `cropped_256`, or `original_256`. The `[split]` values can be `pretrain`, `train`, `val`, `test`, `val_unseen`, `test_unseen`, `key_unseen`, or `other_heldout`. Note that the `val`, `test`, `val_unseen`, `test_unseen`, `key_unseen`, and `other_heldout` altogether are within the evaluation partition of the `original_256` and `cropped_256` image packages.

The `[chunk]` is determined by using the first two or one characters of the MD5 checksum (in hexadecimal) of the `processid`. This method ensures that the chunk name is purely deterministic and can be computed directly from the `processid`. As a result, the `pretrain` split organizes files into 256 directories by using the first two letters of the MD5 checksum of the `processid`. For the `train` and `other_heldout` splits, files are organized into 16 directories using the first letter of the MD5 checksum. The remaining splits do not use chunk directories since each split has less than 50k images.

A1.5 Metadata file

To enrich the metadata of our published dataset, we’ve integrated structured metadata conforming to Web standards. Our dataset’s metadata file is titled **BIOSCAN_5M_Insect_Dataset_metadata**. We’ve provided two versions of this file: one in CSV format (`.csv`) and the other in JSON-LD format (`.jsonld`). Table A3 outlines the fields of the metadata file and the description of their contents.

A2 Dataset features statistics

A2.1 Geographical information

The detailed statistical analysis of the geographical locations where the organisms were collected, representing the habitats of the organisms, is presented in Table A4. This table indicates the number of distinct regions represented by country, province or state, along with their corresponding longitude and latitude. Additionally, Table A4 provides the count of labelled versus unlabelled records, as well as the class imbalance ratio (IR) for each habitat group within the dataset.

The longitude and latitude coordinates indicate that the dataset comprises 1,650 distinct regions with unique geographical locations shown by Table A4. However, a significant portion of the organisms—approximately 73.36%—were collected from the top 70 most populated regions, which represent only 4.24% of the total regions identified by their coordinates.

Figure A1 shows the distinct countries where the organisms were collected on the world map. The majority of the organisms, over 62%, were collected from Costa Rica.

A2.2 Size information

Monitoring organism size is crucial as it can signal shifts in various factors affecting their lives, including food access, nutrition, and climate change [66]. For instance, in humans, limited access to nutrition correlates with a decrease in average height over generations [70], reflecting environmental

Table A3: Table presents fields of the metadata file of BIOSCAN-5M dataset.

	Field	Description	Type
1	processid	An identifier given by the collector.	String
2	sampleid	An identifier given by the collector.	String
3	taxon	Bio.info: Most specific taxonomy rank.	String
4	phylum	Bio.info: Taxonomic classification label at phylum rank.	String
5	class	Bio.info: Taxonomic classification label at class rank.	String
6	order	Bio.info: Taxonomic classification label at order rank.	String
7	family	Bio.info: Taxonomic classification label at family rank.	String
8	subfamily	Bio.info: Taxonomic classification label at subfamily rank.	String
9	genus	Bio.info: Taxonomic classification label at genus rank.	String
10	species	Bio.info: Taxonomic classification label at species rank.	String
11	dna_bin *	Bio.info: Barcode Index Number (BIN).	String
12	dna_barcode *	Bio.info: Nucleotide barcode sequence.	String
13	country	Geo.info: Country associated with the site of collection.	String
14	province_state	Geo.info: Province/state associated with the site of collection.	String
15	coord-lat	Geo.info: Latitude (WGS 84; decimal degrees) of the collection site.	Float
16	coord-lon	Geo.info: Longitude (WGS 84; decimal degrees) of the collection site.	Float
17	image_measurement_value	Size.info: Number of pixels occupied by the organism.	Integer
18	area_fraction	Size.info: Fraction of the original image the cropped image comprises.	Float
19	scale_factor	Size.info: Ratio of the cropped image to the cropped_256 image.	Float
20	inferred_ranks	An integer indicating at which taxonomic ranks the label is inferred.	Integer
21	split	Split set (partition) the sample belongs to.	String
22	index_bioscan_1M_insect	An index to locate organism in BIOSCAN-1M Insect metadata.	Integer
23	chunk	The packaging subdirectory name (or empty string) for this image.	String

*Note for reviewers: For clarity, two fields were renamed between the main paper submission and supplementary data submission. `uri` → `dna_bin`; `nucraw` → `dna_barcode`. These changes will be updated in the main text for the camera-ready version.

Table A4: The statistics for the columns indicating geographical locations where the specimens are collected.

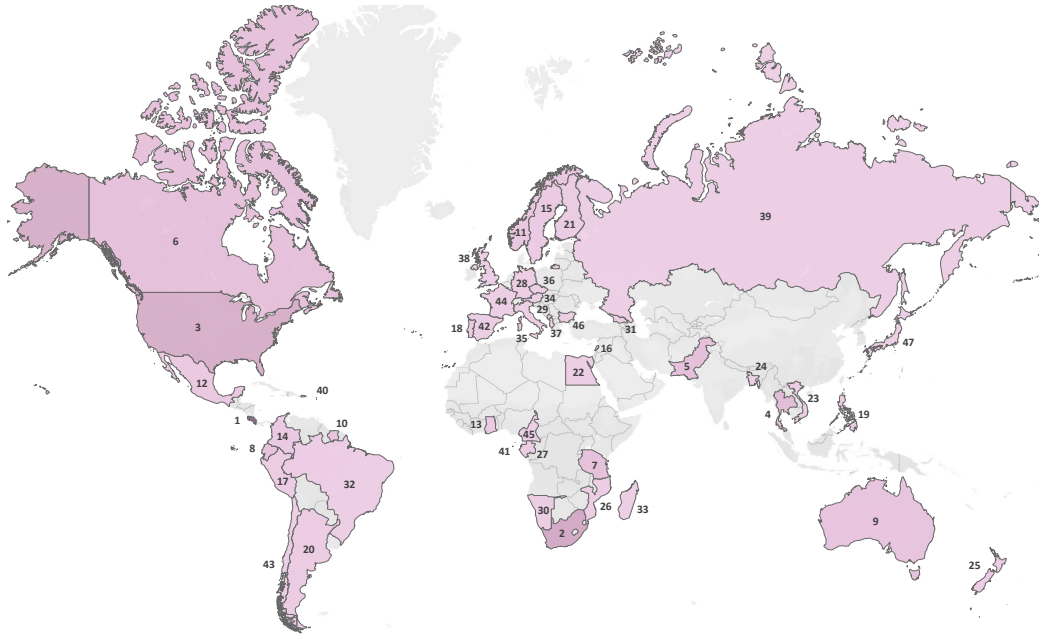
Geo locations	Categories	Labelled	Labelled (%)	Unlabelled	Unlabelled (%)	IR
country	47	5,150,842	100.00	8	0.00	325,631.6
province_state	102	5,058,718	98.21	92,132	1.79	1,243,427.0
coord-lat	1,394	5,149,019	99.96	1,831	0.04	556,352.0
coord-lon	1,489	5,149,019	99.96	1,831	0.04	618,931.0
Location (lat, lon)	1,650	5,149,019	99.96	1,831	0.04	520,792.0

and economic changes. Tracking organism size offers insights into environmental shifts vital for biodiversity conservation [32].

Pixel count The raw dataset provides information about each organism’s size by quantifying the total number of pixels occupied by the organism. This information is provided in the `image_measurement_value` field. Since the image capture settings are consistent for all images, irrespective of scale, as indicated by the organism’s distance to the camera, the number of pixels occupied by the organism should approximate its size. Less than 1% of samples of the BIOSCAN-5M dataset do not have this information. To provide a clearer understanding of the content in the `image_measurement_value` field, Figure A2 displays examples of original images along with their corresponding masks, highlighting the total number of pixels occupied by an organism. To determine the real-world size of the organism based on the number of pixels, it is also important to have the pixel to metric scaling factor. For the original full sized images, most of the images are captured using a Keyence imaging system with a known pixel to millimeter scaling. See §A4.1 for details on the pixel scale and how to determine it for cropped and resized images.

A2.3 Dataset category distribution

For detailed insights into the class distribution within the major categories of the BIOSCAN-5M dataset, Table A5 presents comprehensive statistics. This table provides the total number of categories across 7 taxonomic group levels and BINs, highlighting both the most and least densely populated



1. Costa Rica: 3,256,316	9. Australia: 90,664	17. Peru: 26,656	25. New Zealand: 14,184	33. Madagascar: 4,359	41. Sao Tome and Principe: 356
2. South Africa: 322,096	10. Suriname: 82,842	18. Portugal: 25,780	26. Mozambique: 12,217	34. Austria: 711	42. Spain: 345
3. United States: 281,411	11. Norway: 60,925	19. Philippines: 24,708	27. Gabon: 11,942	35. Italy: 701	43. Chile: 329
4. Thailand: 152,975	12. Mexico: 46,982	20. Argentina: 24,626	28. Germany: 11,310	36. Czech Republic: 515	44. France: 261
5. Pakistan: 126,990	13. Ghana: 38,256	21. Finland: 19,978	29. Montenegro: 10,869	37. Albania: 379	45. Cameroon: 203
6. Canada: 117,599	14. Colombia: 34,444	22. Egypt: 19,841	30. Namibia: 10,278	38. United Kingdom: 376	46. Bulgaria: 33
7. Tanzania: 108,945	15. Sweden: 27,912	23. Vietnam: 16,395	31. Georgia: 9,205	39. Russia: 361	47. Japan: 10
8. Ecuador: 104,676	16. Lebanon: 27,744	24. Bangladesh: 15,352	32. Brazil: 7,427	40. Antigua and Barbuda: 358	

Figure A1: Global distribution of sample collection efforts. The countries are ranked by the number of samples collected.

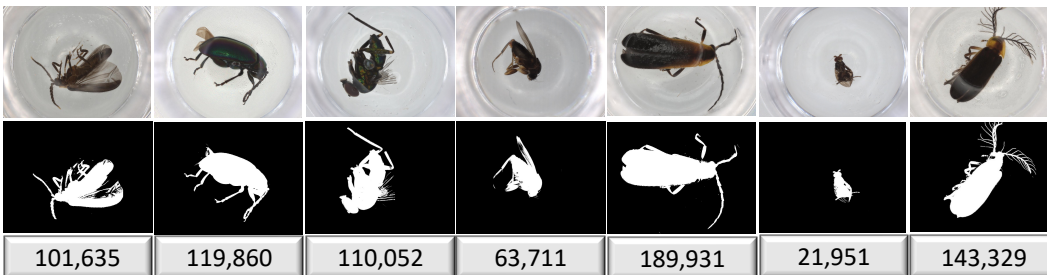


Figure A2: Examples of original images of the BIOSCAN-5M dataset, along with their respective total number of pixels (size) that occupy the image. The top row shows original images and the bottom row shows masks.

ones. Additionally, it includes calculated means, medians, and standard deviations of the population vectors of all sub-categories of each attribute.

Figure A3 illustrates the class distribution within taxonomic rank order, with 99.42% of organisms labelled, approximately 70% are classified as order Diptera.

A2.4 Insect and non-insect organisms

Considering the class Insect the most populated category under taxonomic rank class, the genetic statistics of the dataset is presented in Table A6. Figure A3 illustrates the class distribution within taxonomic rank class, with 99.92% of organisms labelled, where 97.82% belong to the Insect class. Figure A4 shows examples of the original images of non-insect taxonomic classes of the BIOSCAN-5M dataset, with a total of 137,479 organisms.

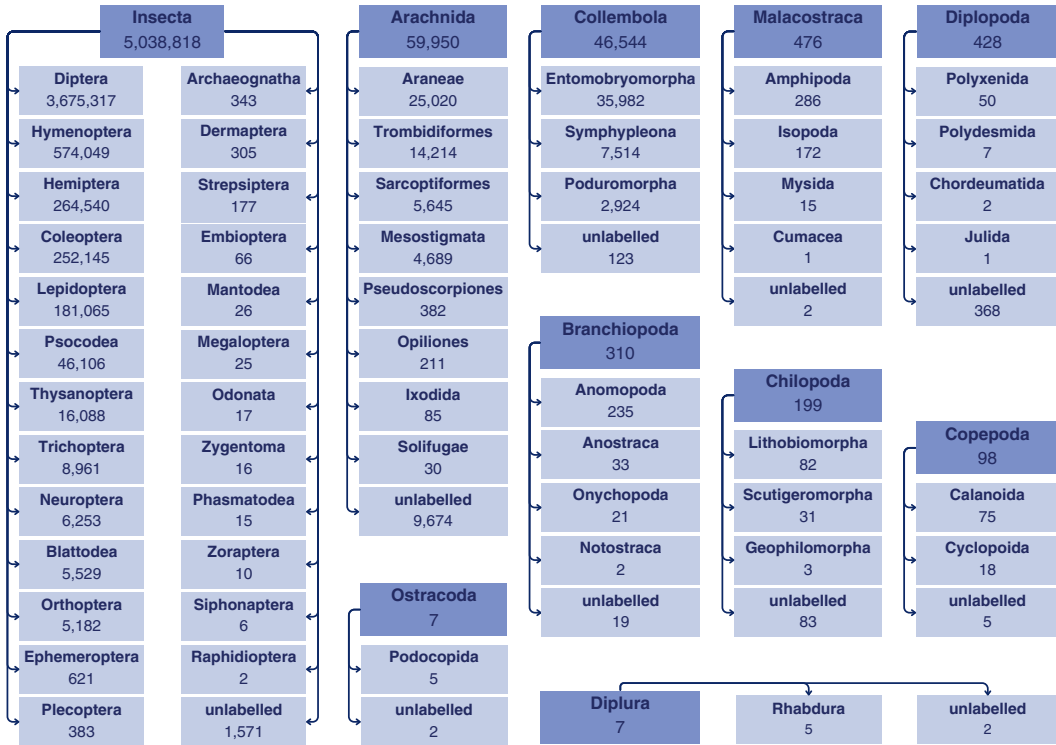


Figure A3: Distribution of taxonomic ranks in the BIOSCAN-5M dataset. Each darker cell represents a taxonomic class, while the lighter cells within each class represent the corresponding taxonomic orders. The numbers indicate the records belonging to each class and order. The *unlabelled* category denotes the number of records that are assigned to a class but not to any specific order.

Table A5: BIOSCAN-5M taxonomic and BIN categories distribution. For each attribute, we show the value which occurs most often in the dataset and the least populated value (in the event of a tie, we show an exemplar selected at random).

Attributes	Categories	Most populated		Least populated		Mean	Median	Std. dev.
		Name	Size	Name	Size			
phylum	1	Arthropoda	5,150,850	Arthropoda	5,150,850	5,150,850.0	5,150,850.0	0.0
class	10	Insecta	5,038,818	Ostracoda	7	514,683.7	369.0	1,508,192.8
order	55	Diptera	3,675,317	Cumacea	1	93,363.4	172.0	495,969.5
family	934	Cecidomyiidae	938,928	Pyrgodesmidae	1	5,281.3	63.5	45,321.1
subfamily	1,542	Metopininae	323,146	Bombyliinae	1	953.7	23.0	9,092.8
genus	7,605	Megaselia	200,268	chalMalaise9590	1	161.3	6.0	2,492.2
species	22,622	Psychoda sp. 11GMK	7,694	Microcephalops sp. China3	1	20.9	2.0	139.5
taxon	28,346	Cecidomyiidae	925,520	Microcephalops sp. China3	1	181.7	3.0	7,101.5
dna_bin	324,411	BOLD:AE01530	35,458	BOLD:ADT1070	1	15.8	2.0	146.4

A3 Limitations and challenges

A3.1 Fine-grained classification

The BIOSCAN-5M dataset provides fine-grained biological features of each organism by annotating images of an organism with multi-grained taxonomic ranks. Additionally, the class imbalance ratio (IR) of each taxonomic group highlights a notable disparity in sample numbers between the majority class (the class with the most samples) and the minority class(es) (those with fewer samples). For example, among the 55 distinct orders, Diptera emerges as the most densely populated order, encompassing approximately 50% of the organisms. Figure A5 presents distinct species from the order Diptera and shows the high similarity between images of different distinct categories. This feature poses further challenges for our downstream classification tasks. We conduct benchmark

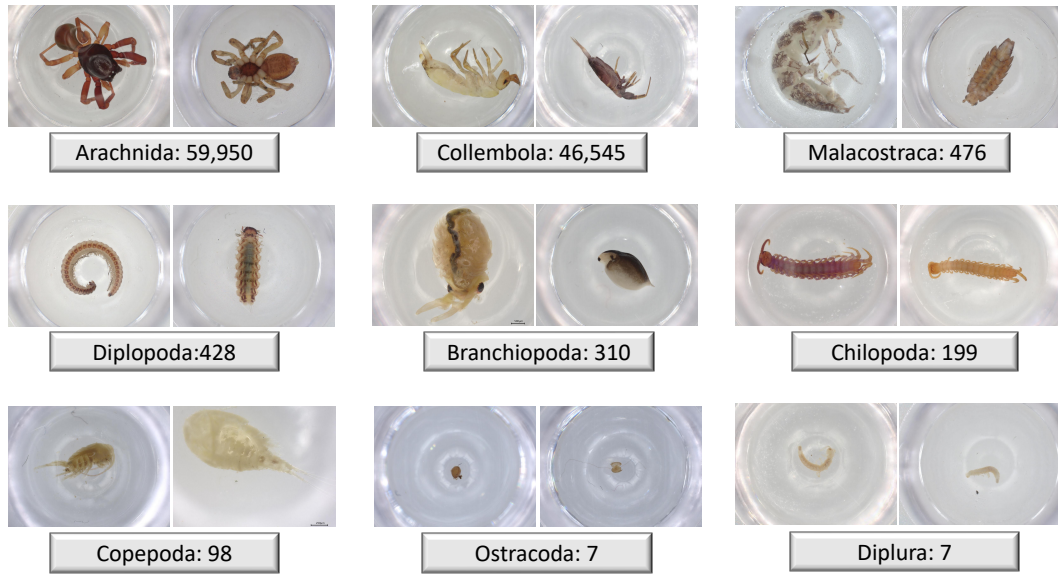


Figure A4: Examples of original images of non-insect class organisms of the BIOSCAN-5M dataset. The name and number below each image denotes the class-level name, and its population within BIOSCAN-5M dataset, respectively.

Table A6: The taxonomic and genetic statistics of class Insecta.

Attributes	Categories	Labelled	Labelled (%)	Unlabelled	Unlabelled (%)	IR
order	25	5,037,247	99.97	1,571	0.03	1,837,658
family	681	4,853,383	96.32	185,435	3.68	938,928
subfamily	1,305	1,431,962	28.42	3,606,856	71.58	323,146
genus	6,897	1,188,043	23.58	3,850,775	76.42	200,268
species	21,512	450,215	8.93	4,588,603	91.07	7,694
taxon	26,603	5,038,818	100.00	0	0.00	925,520
dna_bin	311,743	5,025,921	99.74	12,897	0.26	35,458
dna_barcode	2,423,704	5,038,818	100.00	0	0.00	3,743

experiments focusing on deeper taxonomic level classification, such as genus and species, utilizing both RGB images and textual DNA sequences.

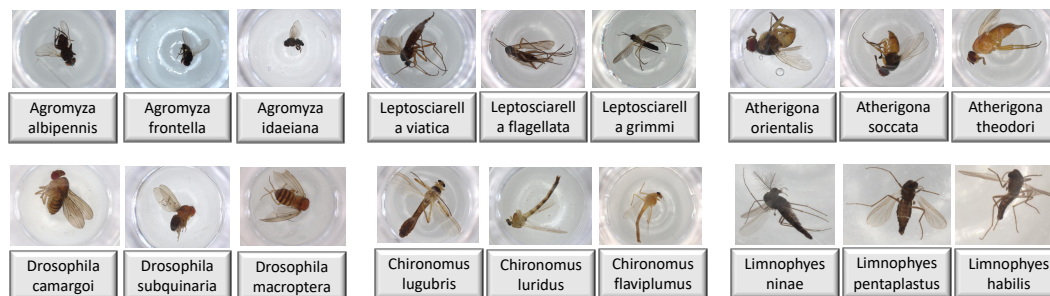


Figure A5: Sample images of distinct species from the Order Diptera, which comprises about 50% of our dataset. High similarity between samples of different species highlights significant classification challenges.

A3.2 Accessing ground-truth labels

The BIOSCAN-5M dataset exposes a limitation regarding labelling. The number of labelled records sharply declines as we delve deeper into taxonomic ranking groups, particularly when moving towards finer-grained taxonomic ranks beyond the family level. In fact, over 80% of the organisms lack taxonomic labels for ranks such as subfamily, genus and species. This circumstance poses a significant challenge for conducting taxonomic classification tasks. However, this limitation also opens doors to opportunities for research in various domains. The abundance of unlabelled data presents avenues for exploration in clustering, unsupervised, semi-supervised, and self-supervised learning paradigms, allowing for innovative approaches to data analysis and knowledge discovery. Leveraging this characteristic, our article delves into zero-shot clustering experiments using embeddings from pretrained self-supervised encoders on the BIOSCAN-5M dataset.

A3.3 Sampling Bias

The BIOSCAN-5M dataset also exposes a sampling bias as a result of the locations where and the methods through which organisms were collected, as depicted by Figure A1.

A4 Data processing

To optimize our benchmark experiments using the BIOSCAN-5M dataset, we implemented two critical pre-processing steps on the raw dataset samples. These steps were necessary to enhance the efficiency and accuracy of our downstream tasks.

The first step involved image cropping and resizing. Due to the high resolution and large size of images in the dataset, processing the original images is both time-consuming and computationally expensive. Additionally, the area around the organism in each image is redundant for our feature extraction. To address these issues, we cropped the images to focus on the region of interest, specifically the area containing the organism. This step eliminated unnecessary background, reducing the data size and focusing the analysis on the relevant parts of the images. After cropping, we resized the images to a standardized resolution, further reducing the computational load and ensuring uniformity across all image samples.

The second step addressed inconsistencies in the taxonomic labels. In the raw dataset, we encountered identical DNA nucleotide sequences labelled differently at certain taxonomic levels, likely due to human error (e.g., typos) or disagreements in taxonomic naming conventions. Such discrepancies posed significant challenges for our classification tasks involving images and DNA barcodes. To address this, we implemented a multi-step cleaning process for the taxonomic labels. We identified and flagged inconsistent labels associated with identical DNA sequences and corrected typographical errors to ensure accurate and consistent naming.

We present additional details of our pre-processing steps in the following section.

A4.1 Image processing details

The BIOSCAN-5M dataset contains resized and cropped images following the process in BIOSCAN-1M Insect [23]. We resized images to 256 px on the smaller dimension. As in BIOSCAN-1M, we opt to conduct experiments on the cropped and resized images due to their smaller size, facilitating efficient data loading from disk.

Cropping. Following BIOSCAN-1M [23], we develop our cropping tool by fine-tuning a DETR [10] model with a ResNet-50 [28] backbone (pretrained on MSCOCO [44]) on a small set of 2,837 insect images annotated using the Toronto Annotation Suite*.

For BIOSCAN-1M, the DETR model was fine-tuned using 2,000 insect images (see Section 4.2 of [23] for details). While the BIOSCAN-1M cropping tool worked well in general, there are some images for which the cropping was poor. Thus, we took the BIOSCAN-1M cropping tool checkpoint, and further fine-tuned the model for BIOSCAN-5M using the same 2,000 images and an additional 837 images that were not well-cropped previously. We followed the same training setup and hyperparameter settings as in BIOSCAN-1M and fine-tuned DETR on one RTX2080 Ti with batch size 8 and a learning rate of 0.0001. Table A7 shows that our model with additional data achieves better cropping performance on an evaluation set of 100 images that were previously poorly

*<https://aidemos.cs.toronto.edu/annotation-suite/>

cropped (NWC-100-VAL). Before cropping, we increase the size of the predicted bounding box by a fixed ratio $R = 1.4$ relative to the tight bounding box to capture some of the image background. If the bounding box extends beyond the image’s edge, we pad the image with maximum-intensity pixels to align with the white background. These processes are the same with [23]. After cropping, we save the cropped-out bounding box.

Table A7: We compare the performance of the DETR model we used for cropping that was trained with the extra 837 images (NWC-837) that were previously not well-cropped to the model used for BIOSCAN-1M. We report the Average Precision (AP) and Average Recall (AR) computed on an additional validation set consisting of 100 images that were not-well cropped previously (NWC-100-VAL), as well as the images (IP-100-VAL + IW-150-VAL) used to evaluate the cropping tool’s model used in BIOSCAN-1M. Our updated model performs considerably better on NWC-100-VAL, while given comparable performance on the original validation set of images.

Dataset	Training data	NWC-100-VAL		IP-100-VAL + IW-150-VAL	
		AP[0.75]	AR[0.50:0.95]	AP[0.75]	AR[0.50:0.95]
BIOSCAN-1M	IP-1000 + IW-1000	0.257	0.485	0.922	0.894
BIOSCAN-5M	IP-1000 + IW-1000 + NWC-837	0.477	0.583	0.890	0.886

Resizing. After cropping the image, we resize the image to 256 pixels on its smaller side while maintaining the aspect ratio ($r = \frac{w}{h}$). As nearly all original images are 1024×768 pixels, our resized images are (nearly all) 341×256 pixels.

Area fraction. The `area_fraction` field in the metadata file indicates the proportion of the original image represented by the cropped image. This factor is calculated using the bounding box information predicted by our cropping tool and serves as an indicator of the organism’s size. Figure A6 displays the bounding boxes detected by our cropping model, which we used to crop images in the BIOSCAN-5M dataset. The area fraction factor is calculated as follows:

$$f_a = \frac{w_c h_c}{w h} \tag{1}$$

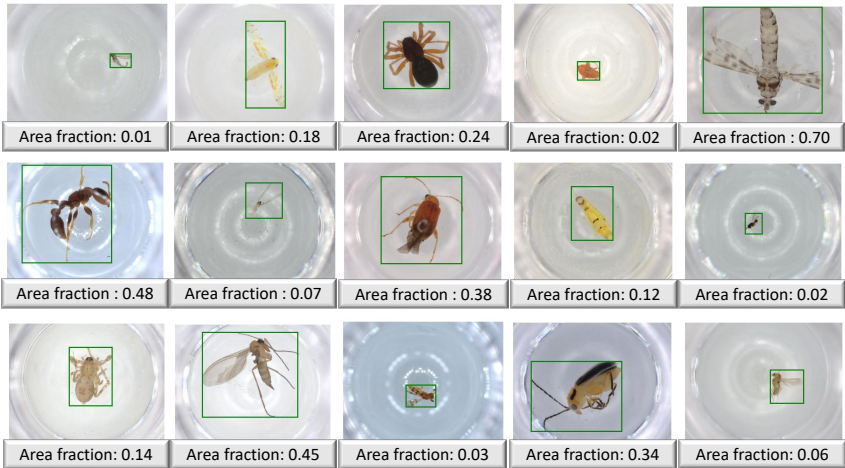


Figure A6: Examples of original images of organisms of the BIOSCAN-5M dataset with the bounding boxes detected by our cropping module. The area fraction value below each image shows how much of the original image is included in the crop.

Scale factor. When capturing images that represent physical objects, such as medical scans or biological samples, the goal is to ensure that measurements taken from the images are accurate representations of the real objects. To be able to compute real-world sizes from the captured images, we require a consistent relationship between pixel size and physical size. Therefore, we added the `scale_factor` field to the metadata file, which determines the ratio of the cropped image to

the cropped and resized (cropped_256) image. Assuming we have the original images (I) with constant width (w) and height (h) for all image samples. The cropped images (I_c), extracted using the bounding box information detected by our cropping tool, have varying widths (w_c) and heights (h_c) proportional to the size of the organism. Finally, the resized images (I_r) are adjusted such that the shorter of the width (w_r) and height (h_r) becomes a constant size of 256 px, with the other dimension scaled proportionally to maintain the aspect ratio, resulting in a size larger than 256 px. We calculated the scale-factor (f_s) as follows:

$$f_s = \frac{\min(w_c, h_c)}{256} \quad (2)$$

If we define the pixel scale as the number of millimeters per pixel, then the pixel scale of the cropped and resized image (cropped_256) is equivalent to the pixel scale of the original image multiplied by the scale factor:

$$\text{pixel_scale}_{\text{cropped_256}} = \text{pixel_scale}_{\text{original}} \times f_s \quad (3)$$

Note the pixel scale of the original image remains unchanged during the cropping process, as cropping only involves cutting out areas around the region of interest (the organism) without scaling the image. The Keyence imaging system used to capture the original 1024×768 images has a resolution of 0.1554 mm (horizontal) \times 0.1554 mm (vertical) per pixel. Using this pixel scale and the scale factor obtained from the cropped image’s width and height, we can estimate the size of the object in the real-world.

A4.2 HDF5 file

To load data efficiently during the training of the BIOSCAN-CLIP baseline, we also generated a 190 GB HDF5 file to store images and related metadata from the BIOSCAN-5M dataset. This file is structured to allow rapid access and processing of large-scale data.

At the top level, the file consists of a *group* of the following *datasets* representing different partitions of BIOSCAN-5M. Each partition includes keys or queries for one or all of the splits (pretraining, validation, or test).

For more information or to download the HDF5 file, the instructions are found at the BIOSCAN-CLIP GitHub repo: <https://github.com/3dlg-hcvc/bioscan-clip>.

A4.3 Taxa of unassigned placement

Some taxonomic labels had “holes” in them due to the complexities of the definition of taxonomic labels. Established taxonomic labels for some species can omit taxonomic ranks because there is currently no scientific need to define a grouping at that taxonomic level.

In particular, we found there were 1,448 genera which were missing a subfamily label because their genus had not been grouped into a subfamily by the entomological community. Note that these genera might at some point in the future be assigned a subfamily, if a grouping of genera within the same family becomes apparent.

This situation of mixed rankings creates a complexity for hierarchical modelling, which for simplicity typically assumes a rigid structure of level across the labelling tree for each sample. We standardized this by adding a placeholder subfamily name where there was a hole, equal to “unassigned <Family_name>”. For example, for the genus *Alpinosciara*, the taxonomic label was originally:

```
Arthropoda > Insecta > Diptera > Sciaridae > [none] > Alpinosciara
```

and after filling the missing subfamily label, it became:

```
Arthropoda > Insecta > Diptera > Sciaridae > unassigned Sciaridae > Alpinosciara
```

This addition ensures that the mapping from genus to subfamily is injective, and labels which are missing because they are not taxonomically defined are not confused with labels which are missing because they have not been identified. Furthermore, this ensures that each subsequent rank in the taxonomic labels provides a partitioning of each of the labels in the rank that proceeds it.

A4.4 Taxonomic label cleaning

The taxonomic labels were originally entered into the BOLD database by expert entomologists using a drop-down menu for existing species, and typed-in manually for novel species. Manual data entry

can sometimes go awry. We were able to detect and resolve some typographical errors in the manual annotations, as described below.

Genus and species name comparison. Since species names take the form “<Genus_name> <species_specifier>”, the genus is recorded twice in samples which possess species labels. This redundancy provides an opportunity to provide a level of quality assurance on the genus-level annotations. A few samples (82 samples across 13 species) had a species label but no genus label; for these we used the first word of the species label as the genus label. For the rest of the samples with a species label, we compared the first word of the species label with the genus label, and resolved 166 species where these were inconsistent. These corrections also uncovered cases where the genus name was entered incorrectly more broadly, and we were able to correct genera values which were entered incorrectly even in cases where they were consistent with their species labels or had no species labels.

Conflicted annotations for the same barcode. We found many DNA barcodes were repeated across the dataset, with multiple images bearing the same barcode. Overall, there were on average around two repetitions per unique barcode in the dataset. It is already well-established that the COI mitochondrial DNA barcode is a (sub)species-level identifier, i.e. same barcode implies same species, and different species implies different barcodes. Hence we have a strong prior that samples with the same barcode should be samples of the same species. This presents another opportunity to provide quality assurance on the data, by comparing the taxonomic annotations across samples which shared a DNA barcode. Differences can either arise by typos during data entry, or by differences of opinion between annotators.

We investigated cases where completed levels of the taxonomic annotations differed for the same barcode. This indicated some common trends as values often compared as different due to stylistic differences, where one annotation differed only by casing, white-space, the absence of a 0 padding digit to an identifier code number, or otherwise misspellings. We resolved some such disagreements automatically, by using the version more common across the dataset.

The majority of placeholder genus and species names follow one of a couple of formats such as “<Genus_name> Malaise1234”, e.g. “*Oxysarcodexia Malaise4749*”. Comparing different taxonomic annotations of the same barcode only allows us to find typos where a barcode has been annotated more than once. However, there are of course more barcodes than species and so there may remain some typos which make two samples of the same species with different barcodes compare as different when they should be the same. To address this, we found labels which deviated from the standardized placeholder name formats and modified them to fit the standardized format. Examples of these corrections include adding missing zero-padding on digits, fixing typos of the word “Malaise”, and inconsistent casing. In this way, we renamed the species of 6,756 samples and genus of 3,675 across 7,673 records.

We resolved the remaining conflicts between differently annotated samples of the same barcode as follows. We considered each taxonomic rank one at a time. In cases where there was a conflict between the annotations, we accepted the majority value if at least 90% of the annotations were the same. If the most common annotation was less prevalent than this, we curtailed the annotation at the preceding rank. Curtailed annotations which ended at a filler value (i.e. a subfamily name of the format “unassigned <Family_name>”) were curtailed at the last completed rank instead. In total, we dropped at least one label from 3,478 records.

Next, we considered barcodes whose multiple annotations differed in their granularity. In such cases, we inferred the annotations for missing taxonomic ranks from the samples that were labelled to a greater degree of detail. In total, we inferred at least one label for 172,895 records. We believe these inferred labels are unlikely to have an error rate notably higher than that of the rest of the data. Even so, we provide details about which ranks were inferred in the metadata field `inferred_ranks` in case the user wishes to exclude the inferred labels. This field takes the following values:

- 0 — Original label only (nothing inferred).
- 1 — Species label was copied. (Sample was originally labelled to genus-level.)
- 2 — Genus and (if present) species were copied.
- 3 — Subfamily, and every rank beneath it, were copied.
- 4 — Family, and every rank beneath it, were copied.

Table A8: Example species from each species set.

Species set	Genus	Species	Number of samples			
			All	Train/ Keys	Val	Test
seen	Aacanthocnema	Aacanthocnema dobsoni	3	3	0	0
	Glyptapanteles	Glyptapanteles meganmiltonae	65	45	2	18
	Megaselia	Megaselia lucifrons	699	640	34	25
	Pseudomyrmex	Pseudomyrmex simplex	378	335	18	25
	Rhopalosiphoninus	Rhopalosiphoninus latysiphon	148	116	7	25
	Stenoptilodes	Stenoptilodes brevipennis	16	10	1	5
	Zyras	Zyras perdecoratus	10	6	0	4
unseen	Anastatus	Anastatus sp. GG28	42	24	6	12
	Aristotelia	Aristotelia BioLep531	87	51	13	23
	Glyptapanteles	Glyptapanteles Whitfield155	11	6	1	4
	Megaselia	Megaselia BOLD:ACN5814	24	13	3	8
	Orthocentrus	Orthocentrus Malaise5315	39	23	5	11
	Phytomyptera	Phytomyptera Janzen3550	14	8	1	5
	Zatypota	Zatypota alborhombartaDHJ03	9	8	1	0
heldout	Basileunculus	Basileunculus sp. CR3	268			
	Cryptophilus	Cryptophilus sp. SAEVG Morph0281	55			
	Glyptapanteles	Glyptapanteles Malaise2871	1			
	Odontofroggata	Odontofroggata corneri-MIC	13			
	Palmistichus	Palmistichus ixtlilxochitliDHJ01	416			
	gelBioLep01	gelBioLep01 BioLep3792	16			
	microMalaise01	microMalaise01 Malaise1237	13			

- 5 — Order, and every rank beneath it, were copied.
- 6 — Class, and every rank beneath it, were copied.

Non-uniquely identifying species names. Finally, we noted that some species names were not unique identifiers for a species. These cases arise where an annotator has used *open nomenclature* to indicate a suspected new species, e.g. “*Pseudosciara sp.*”, “*Olixon cf. testaceum*”, and “*Dacnusa nr. faeroensis*”. Since this is not a uniquely identifying placeholder name for the species, it is unclear whether two instances with the same label are the same new species or different new species. For example, there were 1,247 samples labelled as “*Pseudosciara sp.*”, and these will represent a range of new species within the *Pseudosciara* genus, and not repeated observations of the same new species. Consequently, we removed such species annotations which did not provide a unique identifier for the species. In total, 198 such species values were removed from 5,101 samples.

Conclusion. As a result of this cleaning process we can make the following claims about the dataset, with a high degree of confidence:

- All records with the same barcode have the same annotations across the taxonomic hierarchy.
- If two samples possess a species annotation and their species annotation is the same, they are the same species. (Similarly for genus level annotations, etc.)
- If two samples possess a species annotation and their species annotations differ, they are not the same species. (Similarly for genus level annotations, etc.)

A4.5 Dataset partitioning — Additional details

Species sets. As summarized in §4.1 of the main text, we first partitioned the data based on their species label into four categories as follows:

- *Unknown*: samples without a species label (note: these may truly belong in any of the other three categories).
- *Seen*: all samples whose species label is an established scientific name of a species. Species which did not begin with a lower case letter, contain a period, contain numerals, or contain

“malaise” (case insensitive) were determined to be labelled with a catalogued, scientific name for their species, and were placed in the *seen* set.

- *Unseen*: Of the remaining samples, we considered the placeholder species which we were most confident were labelled reliably. These were species outside the seen species, but the genus occurred in the seen set. Species which satisfied this property and had at least 8 samples were placed in the *unseen* set.
- *Heldout*: The remaining species were placed in *heldout*. The majority of these have a placeholder genus name as well as a placeholder species name, but some have a scientific name for their genus name.

This partitioning ensures that the task that is posed by the dataset is well aligned with the task that is faced in the real-world when categorizing insect samples. Example species for each species set are shown in Table A8, and the number of categories for each taxonomic rank are shown in Table A9.

Table A9: Number of (non-empty) categories for each taxa, per species set.

Species set	phylum	class	order	family	subfamily	genus	species
unknown	1	10	52	869	1,235	4,260	0
seen	1	9	42	606	1,147	4,930	11,846
unseen	1	3	11	64	118	244	914
heldout	1	4	22	188	381	1,566	9,862
overall	1	10	55	934	1,542	7,605	22,622

Splits. To construct partitions appropriate for a closed world training and evaluation scenario, we partitioned the seen data into `train`, `val`, and `test` partitions. Because many of the DNA barcodes have more than one sample (i.e. multiple images per barcode), we partitioned the data at the barcode level. The data was highly imbalanced, so to ensure the `test` partition had high sample efficiency, we flattened the distribution for the `test` set. For each species with at least 2 barcodes and at least 8 samples, we selected barcodes to place in the `test` set. We tried to place a number of samples in the `test` set which scaled linearly with the number of samples for the species, starting with a minimum of 4, and capped at a maximum of 25 (reached at 92 samples total). The target increased at a rate of $1/4$. We capped the number of barcodes to place in the `test` set at a number that increased linearly with the number of barcodes for the species, starting at 1 and increasing at a rate of $1/3$. This flattened the distribution across species in the `test` set, as shown in Figures A7e, A8e, and A9e.

Table A10: Number of (non-empty) categories for each taxa, per partition.

Partition	phylum	class	order	family	subfamily	genus	species
pretrain	1	10	52	869	1,235	4,260	0
train	1	9	42	606	1,147	4,930	11,846
val	1	5	27	350	598	1,704	3,378
test	1	6	27	352	594	1,736	3,483
key_unseen	1	3	11	64	118	244	914
val_unseen	1	3	11	62	116	240	903
test_unseen	1	3	11	62	113	234	880
other_heldout	1	4	22	188	381	1,566	9,862
overall	1	10	55	934	1,542	7,605	22,622

To evaluate model performance during model development cycles, we also created a validation partition (`val`) with the same distribution as the `test` set. This was partition was created to contain around 5% of the remaining samples from each of the seen species, by selecting barcodes to place in the `val` partition. To mimic the long tail of the distribution, for each species with fewer than 20 samples and at least 6 samples, and for which one of their barcodes had only a single image, we added one single-image barcode to the `val` partition. This step added 1,766 individual samples from the tail; for comparison, our target of 5% of the samples from the tail would be 1,955 samples.

The remaining barcodes with samples of seen species are placed in the `train` partition. For retrieval paradigms, we use the `train` partition as keys and the `val` and `test` partitions as queries.

Table A11: Number of species in common between each pair of partitions.

	pretrain	train	val	test	key_unseen	val_unseen	test_unseen	other_heldout
pretrain	0	0	0	0	0	0	0	0
train	0	11,846	3,378	3,483	0	0	0	0
val	0	3,378	3,378	2,952	0	0	0	0
test	0	3,483	2,952	3,483	0	0	0	0
key_unseen	0	0	0	0	914	903	880	0
val_unseen	0	0	0	0	903	903	878	0
test_unseen	0	0	0	0	880	878	880	0
other_heldout	0	0	0	0	0	0	0	9,862

Table A12: Fraction of species (%) in common between each pair of partitions, relative to the number of species for the row.

	pretrain	train	val	test	key_unseen	val_unseen	test_unseen	other_heldout
pretrain	N/A	N/A	N/A	N/A	N/A	N/A	N/A	N/A
train	0.0	100.0	28.5	29.4	0.0	0.0	0.0	0.0
val	0.0	100.0	100.0	87.4	0.0	0.0	0.0	0.0
test	0.0	100.0	84.8	100.0	0.0	0.0	0.0	0.0
key_unseen	0.0	0.0	0.0	0.0	100.0	98.8	96.3	0.0
val_unseen	0.0	0.0	0.0	0.0	100.0	100.0	97.2	0.0
test_unseen	0.0	0.0	0.0	0.0	100.0	99.8	100.0	0.0
other_heldout	0.0	0.0	0.0	0.0	0.0	0.0	0.0	100.0

For the unseen species, we use the same methodology as for the seen species to create and `val_unseen`, with the exception that the proportion of samples placed in the `val_unseen` partition was increased to 20% to ensure it is large enough to be useful. The remaining samples of unseen species are placed in the `keys_unseen` partition. For retrieval paradigms, we use the `keys_unseen` partition as keys and the `val_unseen` and `test_unseen` partitions as queries. For open world evaluation, we train on the `test` partition, without presenting any samples from the unseen species during training, and evaluate on `test_unseen`.

The samples of heldout species are placed in the partition `other_heldout`. The utility of these species varies depending on the model paradigm. In particular, we note that as these species are in neither the seen nor unseen species, they can be used to train a novelty detector without the novelty detector being trained on unseen species.

The samples of unknown species are placed entirely in the `pretrain` partition, which can be used for self-supervised pretraining, or semi-supervised learning.

To aid comparison between the coverage of the partitions, we show the number of species in common between each pair of partitions (Table A11), and the percentage of species in common (Table A12). This is a block-diagonal matrix as species labels do not overlap between species sets. The `train` partition has higher diversity than the `val` and `test` partitions, which each cover less than 30% of the seen species. This is due to the long-tail of the distribution — of the 11,846 species, 7,919 species (two thirds) have 6 or fewer samples, and of these 3,756 species only have a single sample. However, these rare species only constituted a small fraction of the `train` samples—only 17,572 samples are members of species with 6 or fewer samples, which is 6% of the `train` partition. Due to our

Table A13: Number of genera in common between each pair of partitions.

	pretrain	train	val	test	key_unseen	val_unseen	test_unseen	other_heldout
pretrain	4,260	2,372	1,190	1,206	217	214	209	682
train	2,372	4,930	1,704	1,736	244	240	234	519
val	1,190	1,704	1,704	1,517	151	148	145	266
test	1,206	1,736	1,517	1,736	157	154	151	276
key_unseen	217	244	151	157	244	240	234	177
val_unseen	214	240	148	154	240	240	232	175
test_unseen	209	234	145	151	234	232	234	172
other_heldout	682	519	266	276	177	175	172	1,566

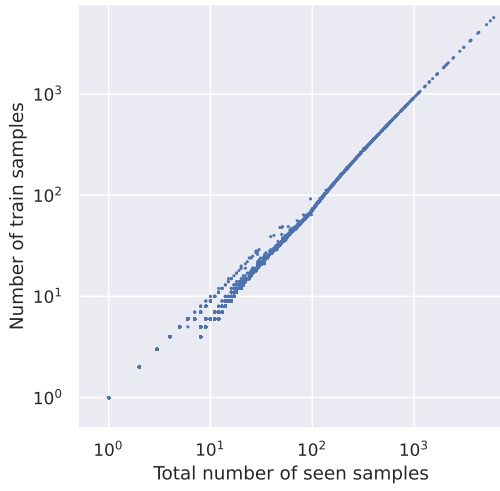
Table A14: Fraction of genera (%) in common between each pair of partitions, relative to the number of genera for the row.

	pretrain	train	val	test	key_unseen	val_unseen	test_unseen	other_heldout
pretrain	100.0	55.7	27.9	28.3	5.1	5.0	4.9	16.0
train	48.1	100.0	34.6	35.2	4.9	4.9	4.7	10.5
val	69.8	100.0	100.0	89.0	8.9	8.7	8.5	15.6
test	69.5	100.0	87.4	100.0	9.0	8.9	8.7	15.9
key_unseen	88.9	100.0	61.9	64.3	100.0	98.4	95.9	72.5
val_unseen	89.2	100.0	61.7	64.2	100.0	100.0	96.7	72.9
test_unseen	89.3	100.0	62.0	64.5	100.0	99.1	100.0	73.5
other_heldout	43.6	33.2	17.0	17.6	11.3	11.2	11.0	100.0

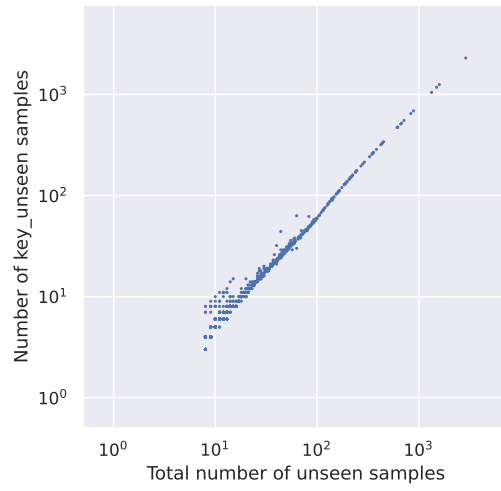
selection process for unseen species, in which only species with enough samples to be confident they are accurate are included, a much higher fraction of the unseen species are included in `val_unseen` and `test_unseen`.

Similarly, we show the number and percentage of genera in common between pairs of partitions (Table A13 and Table A14, respectively). We see that the genera across all seen and unseen species set partitions are contained in the `train` partition.

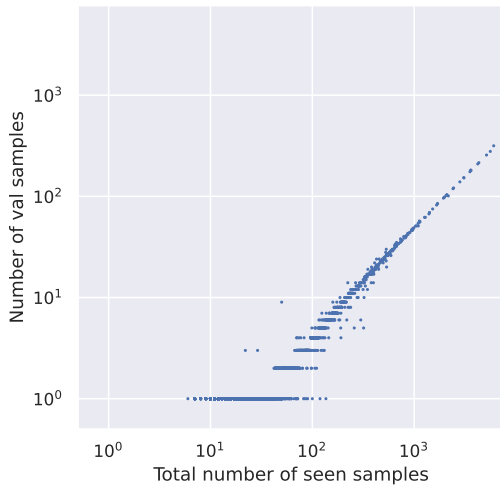
In Figure A10, we show the number of samples per partition. The plot illustrates the vast majority of the samples (91%) are in the `pretrain` partition, and most samples are only labelled to family level (67%).



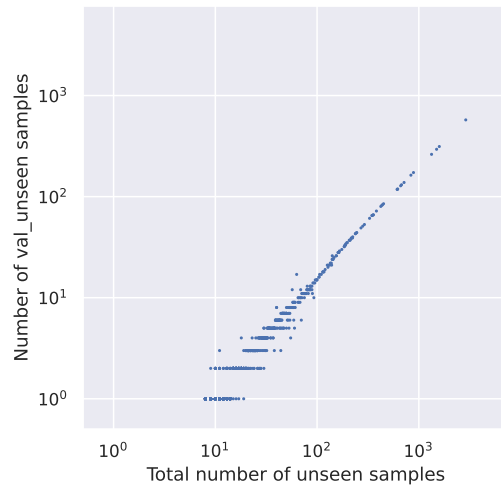
(a) train partition.



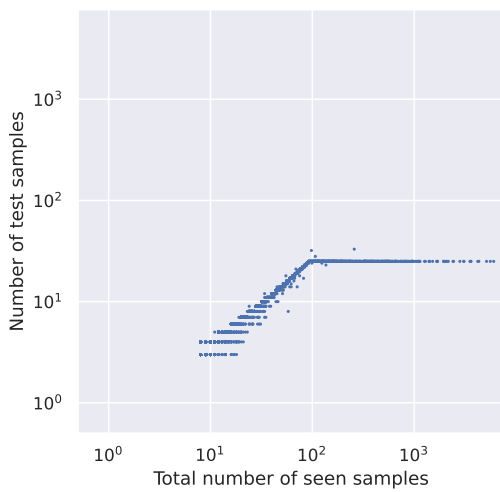
(b) key_unseen partition.



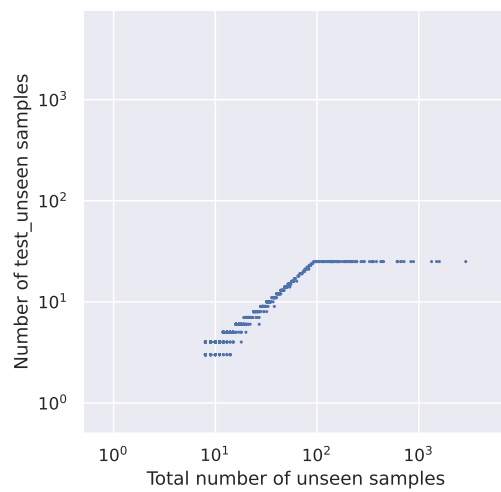
(c) val partition.



(d) val_unseen partition.

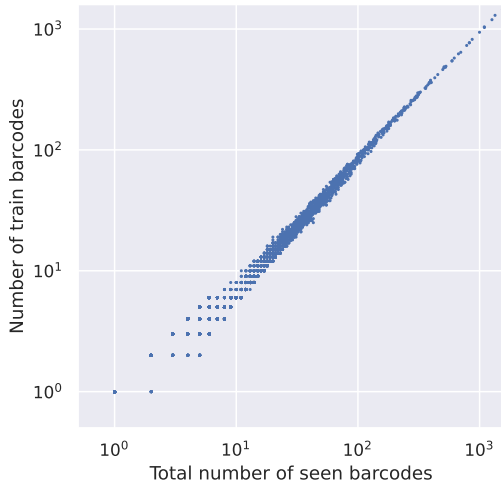


(e) test partition.

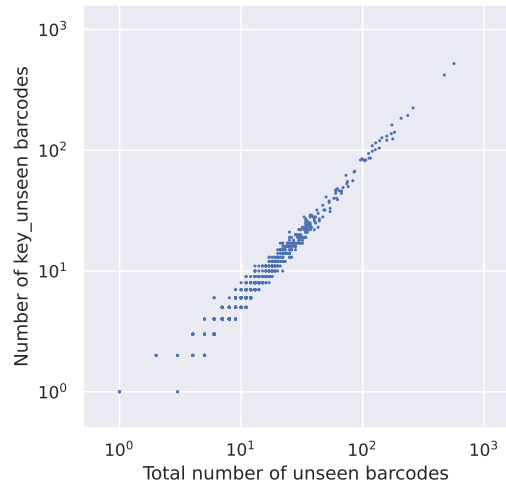


(f) test_unseen partition.

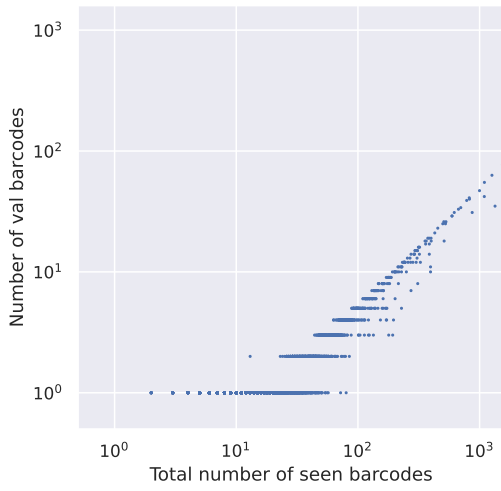
Figure A7: Number of samples in species set and partition, per species.



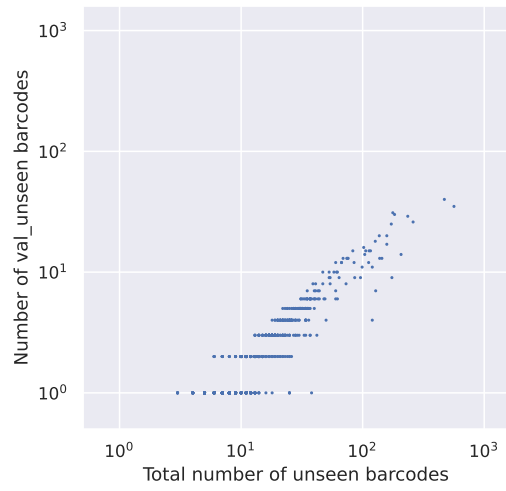
(a) train partition.



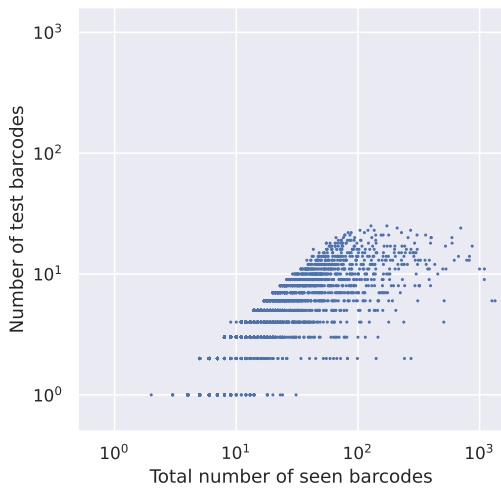
(b) key_unseen partition.



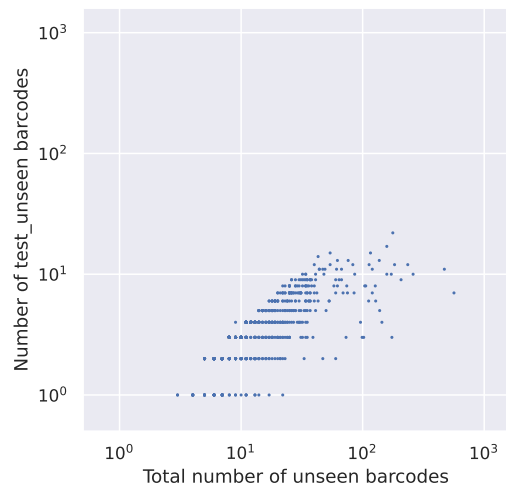
(c) val partition.



(d) val_unseen partition.



(e) test partition.



(f) test_unseen partition.

Figure A8: Number of barcodes in species set and partition, per species.

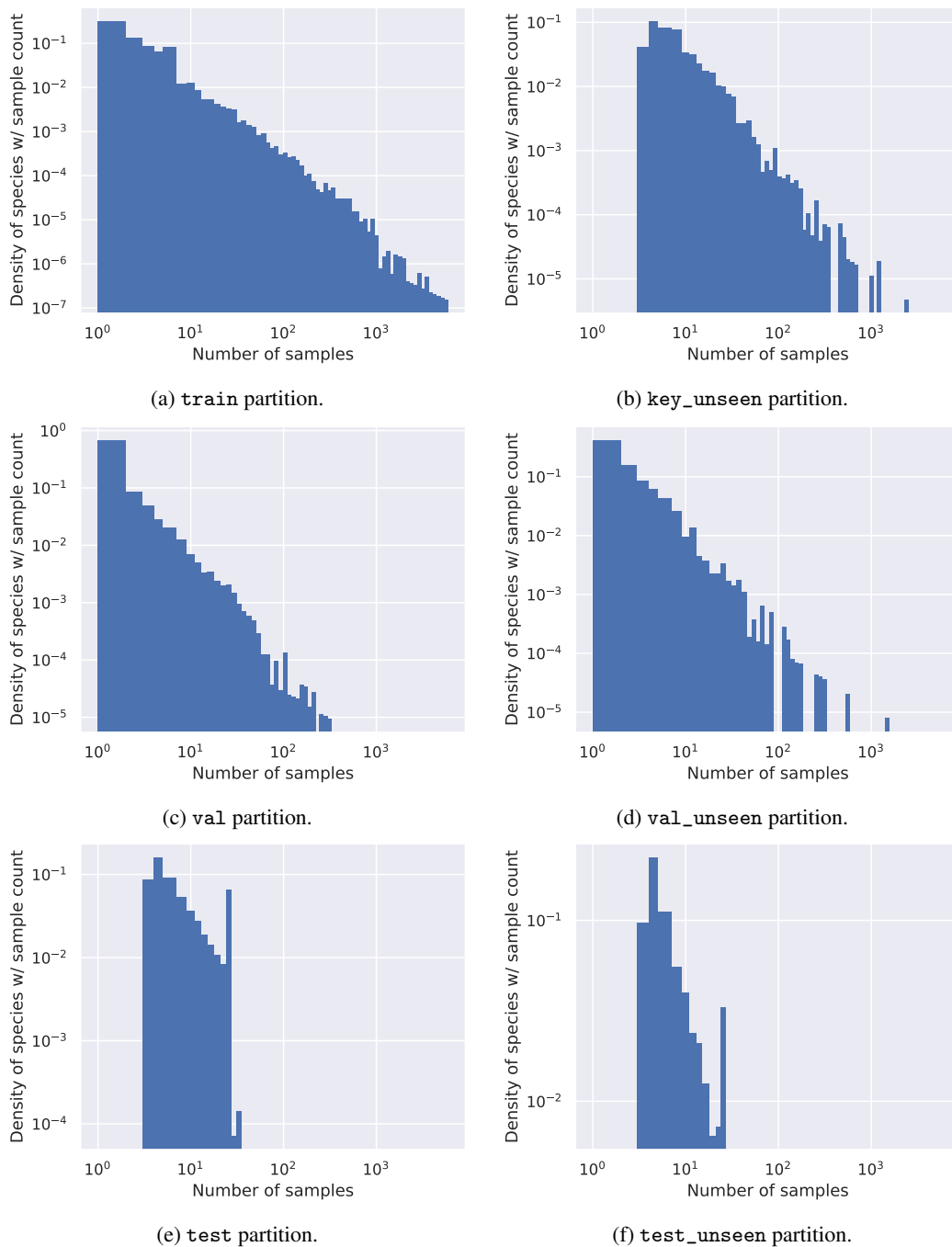


Figure A9: **Distribution of species prevalences across the main data partitions.** Note the log-log axes due to the power law distribution of the data.. The majority of species are infrequent, but some species have many samples. The train and key_unseen partitions have similar distributions to the overall distribution for *seen* and *unseen* species. The val partitions have the same distribution, but shifted left as they they contain a fixed fraction of the samples per species. The test partitions are truncated with a minimum and maximum number of samples per species, which flattens the distribution over species for these partitions.

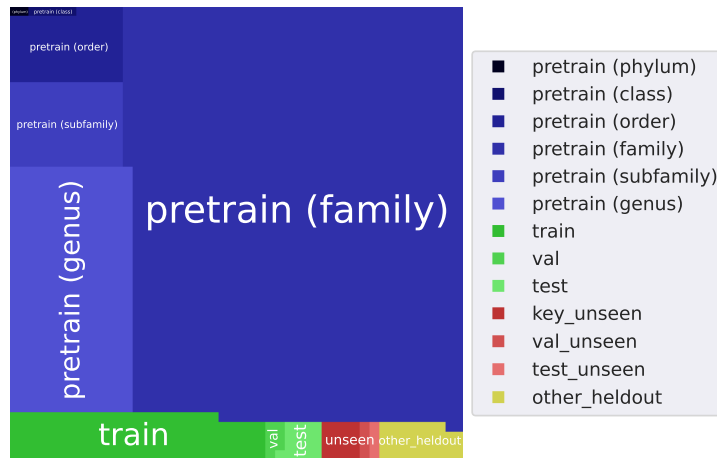


Figure A10: **Area block diagram showing number of samples per partition.** Each square in the 48×48 plot represents 2,236 samples within the dataset of 5 M images and DNA barcodes. For the `pretrain` partition (blues), we provide a further breakdown indicating the most fine-grained taxonomic rank that is labelled for the samples. For the remainder of the partitions (all of which are labelled to species level) we show the number of samples in the partition. Samples for seen species are shown in shades of green, and unseen in shades of red.

A5 DNA-based Taxonomic Classification — Additional Experiments

As described in the main text (§4.2), we leverage all data splits in the BIOSCAN-5M dataset by adopting a semi-supervised learning approach. Specifically, we train a model using self-supervision on the unlabelled partition of the data, followed by fine-tuning on the train split. Our experimental setup is illustrated in Figure 4.

A5.1 Pretraining details

We pretrain the model on the 2,283,900 unique DNA sequences from the `pretrained` partition and the 41,232 unique sequences from the `other_heldout` partition, totalling 2,325,132 pretraining DNA samples. For all samples, trailing N characters are removed and all sequences are truncated at 660 nucleotides. Note that leading N characters are retained since they are likely to correspond to true unknown nucleotides in the barcode. The model was pretrained using the same MLM loss function and training configurations as in BarcodeBERT [52]. Specifically, we use a non-overlapping k -mer-based tokenizer and a transformer model with 12 transformer layers, each having 12 attention heads. However, we included a random offset of at most k nucleotides to each sequence as a data augmentation technique to enhance the sample efficiency. We use a learning rate of 2×10^{-4} , a batch size of 128, a OneCycle scheduler [67], and the AdamW optimizer [46], training the model for 35 epochs. In addition to using the architecture reported in BarcodeBERT, we performed a parameter search to determine the optimal k -mer tokenization length and model size, parameterized by the number of layers and heads in the transformer model, in order to identify an optimal architecture configuration. After pretraining, we fine-tuned the model with cross-entropy supervision for species-level classification. The pre-training stage takes approximately 50 hours using four Nvidia A40 GPUs and the fine-tuning stage of the 4-12-12 models takes 2.5 hours in four Nvidia A40 GPUs.

A5.2 Baseline Models

There has been a growing number of SSL DNA language models proposed in recent literature, most of which are based on the transformer architecture and trained using the MLM objective [38, 85, 86]. These models differ in the details of their model architecture, tokenization strategies, and training data but the underlying principles remain somewhat constant. An exception to this trend is the HyenaDNA [56] model, which stands out by its use of a state space model (SSM) based on the Hyena architecture [60] and trained for next token prediction. For evaluation, we utilized the respective pre-trained models from Huggingface ModelHub, specifically:

- DNABERT-2: `zhihan1996/DNABERT-2-117M`
- DNABERT-S: `zhihan1996/DNABERT-S`
- NT: `InstaDeepAI/nucleotide-transformer-v2-50m-multi-species`
- HyenaDNA: `LongSafari/hyenaDNA-tiny-1k-seqlen`

The BarcodeBERT implementation was taken from <https://github.com/Kari-Genomics-Lab/BarcodeBERT>. All the models, including our pretrained models, were fine-tuned for 35 epochs with a batch size of 32 or 128 and a learning rate of 1×10^{-4} per 64 samples in the batch with the OneCycle LR schedule [67].

A5.3 Linear probe training

A linear classifier is applied to the embeddings generated by all the pretrained models for species-level classification. The parameters of the model are learned using stochastic gradient descent with a constant learning rate of 0.01, momentum $\mu = 0.9$ and weight $\lambda = 1 \times 10^{-5}$.

For the hyperparameter search, shown in Table A15, our linear probe is performed using the same methodology as the fine-tuning stage, except the encoder parameters are frozen.

Table A15: Search over the space of k -mer tokenization length and transformer architectures (number of layers and heads). For fine-tuned and linear probe, we show the class-balanced accuracy (%) on the closed-world val partition, and for 1-NN probe, we show the class-balanced accuracy on the val_unseen partition. Bold: architecture with highest accuracy for the row. Underlined: second highest accuracy.

Evaluation	4 layers, 4 heads				6 layers, 6 heads				12 layers, 12 heads			
	$k=2$	$k=4$	$k=6$	$k=8$	$k=2$	$k=4$	$k=6$	$k=8$	$k=2$	$k=4$	$k=6$	$k=8$
Fine-tuned	93.8	97.8	<u>98.7</u>	98.9	92.4	97.9	49.4	<u>98.7</u>	93.8	98.1	0.0	0.0
Linear probe	32.2	<u>79.8</u>	76.4	97.1	34.3	58.9	8.9	<u>79.7</u>	16.4	3.2	0.0	0.0
1-NN	43.1	50.7	35.0	<u>46.4</u>	46.2	37.2	23.4	37.9	29.1	28.3	0.0	0.1

A6 Zero-Shot Clustering — Additional Experiments

As described in §4.3, we performed a series of zero-shot clustering experiments to establish how pre-trained image and DNA models could handle the challenge of grouping together repeat observations of novel/unseen species. Our methodology is illustrated in Figure 5.

A6.1 Experiment resources

All zero-shot clustering experiments were performed on a compute cluster with the job utilizing two CPU cores (2x Intel Xeon Gold 6148 CPU @ 2.40GHz) and no more than 20 GB of RAM. The typical runtime per experiment was around 4.5 hours.

A6.2 Accounting for Duplicated DNA Barcode Sequences

In our main experiments, we found the performance of DNA-embedding clusterings greatly outperformed that of image-embeddings. However, it is worth considering that there are fewer unique DNA barcodes than images. The mean number of samples per barcode is around two. This provides clustering methods using DNA with an immediate advantage as some stimuli compare as equal and are trivially grouped together, irrespective of the encoder.

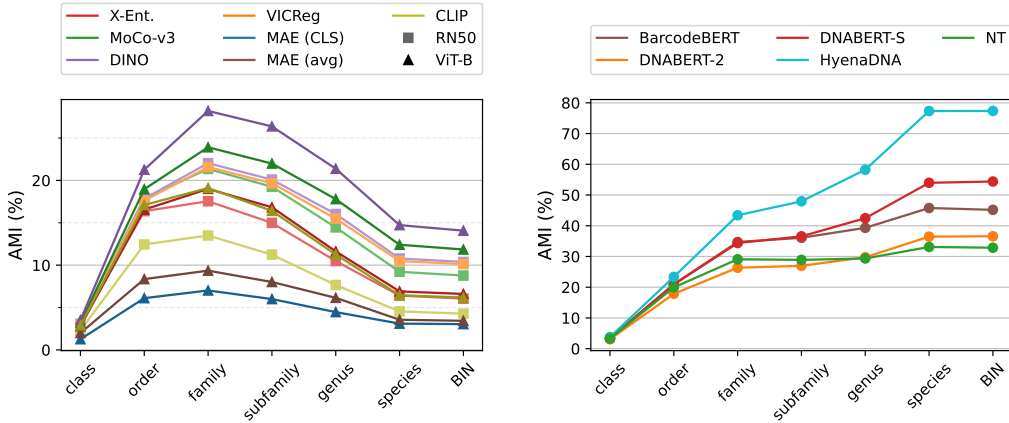


Figure A11: **Zero-shot clustering** AMI (%) performance across taxonomic ranks on test and test_unseen data, with **one sample per barcode**.

To account for this, we repeated our analysis with only one sample per barcode. Our results, shown in Figure A11, indicate that both image and DNA based clusterings are reduced in performance when the number of samples per barcode is reduced to one. This is explained in part by the fact that many species will be reduced to a single observation, which is challenging for clusterers to handle. We found that the performance of most DNA-encoders fell by around half (e.g. from 80% to 40% AMI) when the number of samples per barcode was reduced to one. However the best-performing DNA-encoder, HyenaDNA, was not greatly affected, with its performance reduced from 90% to 80% AMI on the harder clustering task.

Table A16: **Cross-modal zero-shot clustering** AMI (%) performance, on `test` and `test_unseen` data, with **one sample per barcode**.

Architecture	Image encoder	<i>Image-only</i>	DNA encoder				NT
			BarcodeBERT	DNABERT-2	DNABERT-S	HyenaDNA	
—	<i>DNA-only</i>	—	47	52	<u>63</u>	81	36
ResNet-50	X-Ent.	5	30	26	32	9	12
	MoCo-v3	8	29	23	27	11	11
	DINO	<u>11</u>	31	28	31	15	14
	VICReg	10	30	26	30	13	13
	CLIP	6	25	21	25	9	9
ViT-B	X-Ent.	7	33	35	42	13	14
	MoCo-v3	<u>13</u>	38	43	49	21	20
	DINO	15	38	45	<u>51</u>	23	21
	MAE (CLS)	5	33	33	40	10	13
	MAE (avg)	3	29	26	32	7	9
	CLIP	7	34	37	44	14	16

A6.3 Cross-modal embedding clustering

We additionally considered the effect of clustering the embeddings from both modalities at once, achieved by concatenating an image embedding and a DNA embedding to create a longer feature vector per sample. As shown in Table A16, we find that combining image features with DNA features results in a worse performance at species-level clustering.

In preliminary experiments (not shown) we found that the magnitude of the vectors greatly impacted the performance, as large image embeddings would dominate DNA embeddings with a smaller magnitude. We considered standardizing the embeddings before concatenation with several methods (L2-norm, element-wise z-score, average z-score) and found element-wise z-score gave the best performance, a step which we include in these results. Even with this, the performance falls when we add image embeddings to the DNA embeddings. We note that the best DNA-only encoder, HyenaDNA, has the largest drop in performance, which we hypothesise is because it has the shortest embedding dimensions of 128 compared with NT (512-d) and the BERT-based models (768-d).

A7 Multi-Modal Learning — Additional Experiments

As described in §4.4, we trained a multimodal model with an aligned embedding space across the images, DNA, and taxonomic labels. Our methodology is illustrated in Figure 7.

A7.1 Model training and inference

We demonstrate our model training and inference methodology in Figure 7. We use contrastive learning to fine-tune the image, DNA, and text encoders. During inference, we compare the embedding of the query image or DNA input to a key database of embeddings from images, DNA, or taxonomy labels using cosine similarity, and we predict the query’s taxonomy based on the taxonomy of the closest retrieved key embeddings.

A7.2 Additional experiments

We additionally report the micro accuracy in Table A17 to represent performance when averaged over individual samples rather than classes. The results show similar trends to the macro accuracy, with the model trained on the BIOSCAN-5M dataset performing best for broader taxa, especially in image-to-image and image-to-DNA inference setups. Results are more mixed at the species level due in part to the challenge of species classification, highlighting the importance of further research at this fine-grained level.

Table A17: Top-1 micro accuracy (%) on the test set for using different pre-train datasets (BIOSCAN-1M, BIOSCAN-5M) and different combinations of aligned embeddings (image, DNA, text) during contrastive training. We show results for using image-to-image, DNA-to-DNA, and image-to-DNA query and key combinations. As a baseline, we show the results prior to contrastive learning (no alignment). We report the accuracy for seen and unseen species, and the harmonic mean (H.M.) between these (bold: highest acc.).

Taxon	Trained on	Aligned embeddings			DNA to DNA			Image to Image			Image to DNA		
		Img	DNA	Txt	Seen	Unseen	H.M.	Seen	Unseen	H.M.	Seen	Unseen	H.M.
Order	—	✗	✗	✗	98.9	99.3	99.1	94.2	97.0	95.6	18.3	14.7	16.3
	BS-1M	✓	✓	✓	99.9	100.0	99.9	98.2	99.0	98.6	88.5	96.1	92.1
	BS-5M	✓	✓	✗	99.9	100.0	99.9	98.6	99.3	98.9	95.8	97.9	96.8
	BS-5M	✓	✓	✓	99.9	100.0	99.9	98.7	99.3	99.0	96.5	98.3	97.4
Family	—	✗	✗	✗	96.5	97.3	96.9	72.9	76.0	74.4	1.7	1.9	1.8
	BS-1M	✓	✓	✓	99.0	99.0	99.0	89.5	91.1	90.3	66.6	74.5	70.4
	BS-5M	✓	✓	✗	98.2	97.7	98.0	89.7	91.5	90.6	74.0	73.2	73.6
	BS-5M	✓	✓	✓	99.2	99.4	99.3	90.1	91.9	91.0	76.6	79.5	78.0
Genus	—	✗	✗	✗	94.0	93.5	93.7	47.8	47.0	47.4	0.2	0.0	0.1
	BS-1M	✓	✓	✓	95.4	92.4	93.9	71.3	73.3	72.2	27.8	31.4	29.5
	BS-5M	✓	✓	✗	90.7	84.5	87.5	72.1	73.7	72.9	35.2	25.1	29.3
	BS-5M	✓	✓	✓	94.8	91.7	93.2	71.8	71.8	71.8	34.2	28.7	31.2
Species	—	✗	✗	✗	91.6	84.8	88.1	31.9	19.1	23.9	0.0	0.0	0.0
	BS-1M	✓	✓	✓	91.2	72.2	80.6	55.8	40.8	47.2	8.9	4.7	6.1
	BS-5M	✓	✓	✗	83.2	54.7	66.0	56.3	40.0	46.8	14.4	4.2	6.5
	BS-5M	✓	✓	✓	89.6	69.4	78.2	55.9	38.2	45.4	12.5	3.5	5.5

A7.3 Retrieval examples

Figure A12 shows image retrieval examples using images as queries and DNA as keys. These demonstrate the ability of the model to classify taxonomy based on retrieval and the visual similarities of the retrieved images corresponding to the most closely matched DNA embeddings.

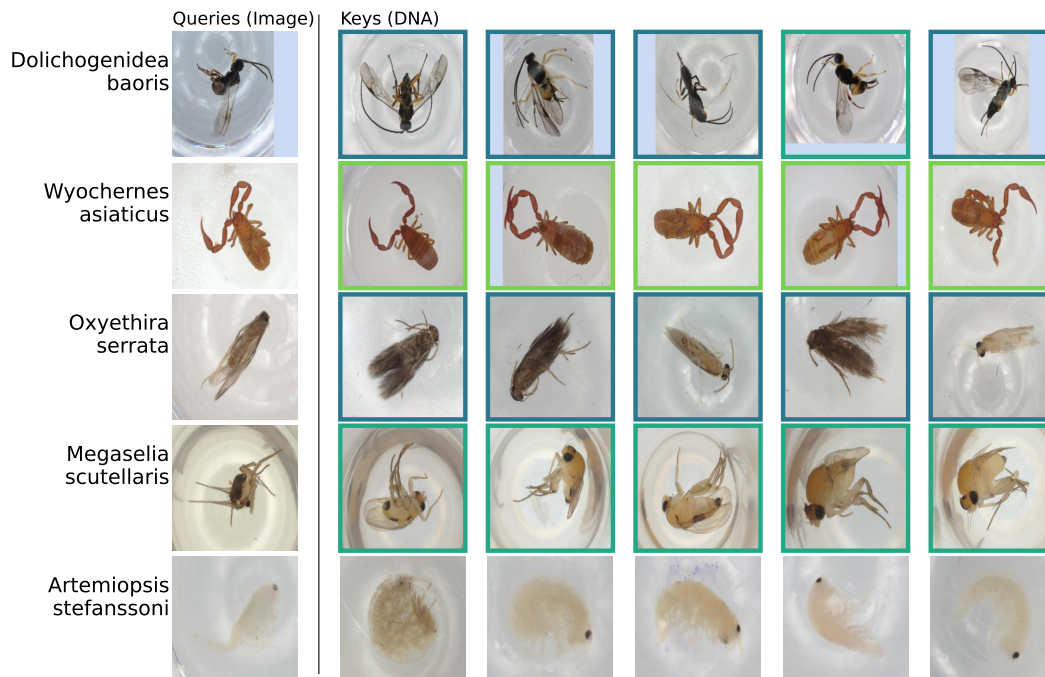


Figure A12: *Example image query-key pairs.* For five distinct query images, we show the top-5 nearest specimens from the test-key dataset retrieved based on the cosine-similarity between the image query and DNA keys, using the BIOSCAN-5M model trained on all three modalities. Surrounding boxes denote keys of the same species (light green), same genus (turquoise), or same family (blue) as the query.